Winter 12-8-2022

INVESTIGATING THE CONTRIBUTION OF MARINE VIRUSES TO OPTICAL BACKSCATTER IN THE <0.2 µM FRACTION OF SEAWATER

Kacey Mae Lange

INVESTIGATING THE CONTRIBUTION OF MARINE VIRUSES TO OPTICAL BACKSCATTER IN THE <0.2 μM FRACTION OF SEAWATER

by

Kacey Mae Lange

A Thesis
Submitted to the Graduate School,
the College of Arts and Sciences
and the School of Ocean Science and Engineering
at The University of Southern Mississippi
in Partial Fulfillment of the Requirements
for the Degree of Master of Science

Approved by:

Dr. Kristina Mojica, Committee Chair
Dr. Xiaodong Zhang
Dr. Christopher Hayes

December 2022

Published by the Graduate School

ABSTRACT

Marine viruses are the smallest and most abundant biological entities in the ocean. Marine viruses play a significant role in carbon and nutrient cycles through the liberation of dissolved organic matter (DOM) through the lysis of their numerically dominant hosts (i.e. bacteria and phytoplankton). Despite their importance, little is known about how viruses contribute to seawaters inherent optical properties (IOP) of seawater, specifically backscatter. All particles produce backscatter, with their contribution dependent on particle size, concentration, and composition. Living particles contribute 10-20% of the total backscatter with the remaining 80% of unclassified backscatter, "missing backscatter", contributed by submicron particles (<1.0 μm), which include viruses and DOM. The backscatter of viruses has never been directly measured in situ before this study. Directly measuring the backscatter contributed by viruses would help to address the gap in our understanding of the composition of the missing backscatter and potentially lead to the use of remote sensing in determining the abundance of viruses in the ocean.

Seawater samples were collected on the STRATIPHYT-21 cruise over a latitudinal transect from 15°N to 35°N at 26°W from the euphotic zone and in three areas of the Gulf of Mexico (Petit Bois, Horn Island, Cat Island). Samples were subjected to two size fractionations (0.2 μm, and 30 kDa) where marine viruses are assumed present in the <0.2 μm filtrate (dissolved fraction), and a significant amount are removed in the 30 kDa filtrate (ultralow molecular weight DOM a.k.a. ULMW DOM fraction). The backscatter of filtrates was compared to elucidate the contribution of viral particles to optical backscatter in the virus fraction (V_f or 0.2 μm – 30 kDa) of seawater. When

examining the contribution of virus scattering to the dissolved fraction of seawater, virus scattering contributes, on average, 50% of the dissolved fraction backscatter. This study demonstrates the potential of viruses to contribute to the backscatter of the dissolved fraction and begins to fill in the gap in our understanding of the “missing backscatter”.

ACKNOWLEDGMENTS

I would like to thank my advisors, Dr. Kristina Mojica and Dr. Xiaodong Zhang, and my committee member Dr. Christopher Hayes. I would also like to thank the STRATIPHYT-21 science members, Dr. Corina Brussard, Anna Noordeloos, and Kirsten Koojiman for sample and data collection and Tonke Bogt, Robin Blonk, and Anne Mol for last-minute participation in the cruise and for sample and data collection and Dr. Kevin Dillon for sharing his lab and instruments. In addition, I would like to thank the Pre-PACE crew for sample collection in the Gulf of Mexico and their support. I appreciate the input and encouragement I received from the following colleagues regarding this work: Sarah Monica, Nick Gagliano, and Corey Pagart. I would also like to thank the captain, and crew of the R/V Pelagia STRATIPHYT-21 North Atlantic transect, and the R/V Jim Franks for the Gulf of Mexico experiment for making this project possible.

DEDICATION

I would like to dedicate this work to my loved ones. Thank you to my family, Ralph Lange, Wendy Lange, Carly Lange, Marcia Krawjeski, Ron Krawjeski, and Phyllis Petrella for encouraging me to chase my dreams, helping me out when I needed it most, and always greeting me with open arms when I return home. I would also like to thank my friends, Sarah Monica, Jordan Zeairs, Nick Gagliano, and Seth Figueroa for always listening to me and for your support. You made this experience enjoyable and made the 45-minute commute worth it. All of you helped me along the way and played a significant role in making this work possible.

TABLE OF CONTENTS

LIST OF TABLES

LIST OF ILLUSTRATIONS

LIST OF ABBREVIATIONS

βbp	Particulate backscattering coefficient
$\beta_{(100)}$	Proxy used for the particulate backscattering coefficient
$\beta_{Dissolved}$	$\beta_{(100)}$ for the dissolved fraction
$\beta_{ULMW\ DOM}$	$\beta_{(100)}$ for the ULMW DOM fraction
β_{Virus}	$\beta_{(100)}$ for the virus fraction
β_{vA}	$\beta_{(100)}$ of ideal GOM virus fraction
β_{vB}	$\beta_{(100)}$ of non-ideal GOM virus fraction
CDOM	Colored Dissolved Organic Matter
Dissolved Fraction	<0.2 µm; includes viruses
DOM	Dissolved organic matter
DOC	Dissolved Organic Carbon
EM	Electron microscopy
FCM	Flow Cytometry
FDOM	Fluorescent Dissolved Organic Matter
GOM	Gulf of Mexico
HCl	Hydrochloric Acid
HMW DOM	High Molecular Weight DOM
IOP	Inherent Optical Properties
MWCO	Molecular Weight Cutoff
NA	North Atlantic
QSU	Quinine Sulfate Unit

TFF	Tangential Flow Filter
ULMW DOM	Ultra Low Molecular Weight Dissolved Organic Matter
	<30 kDa; removes viruses
V_f	Virus fraction
	0.2 µm – 30 kDa
V_{fA}	Ideal GOM virus fraction
V_{fB}	Non-ideal GOM virus fraction
VSF	Volume Scatter Function
$VSF_{Dissolved}$	VSF of the dissolved fraction
$VSF_{D\ Corrected}$	VSF of the corrected dissolved fraction
$VSF_{GOM\ B}$	VSF of the GOM bacteria
$VSF_{ULMW\ DOM}$	VSF of the ULMW DOM fraction
VSF_b	VSF of bacteria
VSF_{Virus}	VSF of viruses
$\%\beta_{Virus}$	Percent contribution viruses have in the dissolved fraction

CHAPTER I - INTRODUCTION

1.1 Importance of Marine Viruses

Marine viruses are the smallest (average sizes ranging 20-300 nm), and most abundant (average abundance in surface seawater of ~10^7 mL^{-1}) biological entity in the ocean, exceeding the abundance of bacteria by approximately 15-fold (Suttle 2007). Marine viruses play a significant role in carbon and nutrient cycles through the lysis of bacteria and phytoplankton (Brussaard et al. 2008). As viruses are an important component of dissolved organic matter (DOM) in the ocean, it is likely they could be optically significant (Wommack and Colwell 2000; Weinbauer 2004; Wigington et al. 2016).

In remote sensing, phytoplankton dynamics have been explored for ~30 years using ocean color to determine global chlorophyll-a concentrations (Bracher et al. 2017). Virus dynamics have only been studied in the field in snapshots (only in certain areas, at certain times), even though their dynamics may be variable with global-scale processes.

1.2 Remote Sensing in Biological Oceanography

Inherent optical properties (IOP) are the absorption and scattering characteristics of particulate and dissolved materials in the ocean (Mobley et al. 2022). The absorption coefficient describes how a volume of matter absorbs light and the volume scattering function (VSF) describes how a volume of matter scatters light. Optics typically measures the alterations in the visible light spectrum of solar radiation to understand how light interacts with living and non-living organic and inorganic particles, specifically in open ocean conditions. Remote sensing relies on backscattered light (i.e. natural light

deflected from 90-180°) from marine constituents to return the incident sunlight to the sensors and hence can be used to derive the characteristics of said constituents (Stramski et al. 2004). Typically, constituents in the ocean are operationally separated into particulate (retained on a 0.2 μm filter) and dissolved (pass through a 0.2 μm filter) (Zhang et al. 2020).

All particles produce backscatter, with their contribution to total backscatter dependent on particle size, concentration, and composition. Living particles, such as phytoplankton and bacteria, and non-living particles, such as DOM and viruses, alter the optical properties of the water column. The use of optics to study the biological particles in the ocean provides an alternate yet effective means of understanding biological-physical interactions (Dickey and Falkowski 2002). It is estimated that living organisms such as phytoplankton, bacteria, flagellates, and ciliates produce a relatively small fraction of particulate backscattering (10-20%), with heterotrophic bacteria being the major contributor of 10-50% of the total particulate backscattering and 5-20% of total backscattering in oligotrophic waters (Stramski and Kiefer 1991; Stramski et al. 2004; Morel and Ahn 2008). The remaining 80% of the total backscatter may be contributed by particles in the submicron (<1.0 μm) size range. Currently, a large percentage of unclassified backscatter is known as ‘missing backscatter’ contributed by submicron particles. These submicron constituents could be important to optical measurements as their abundance is higher than suspended particles (Stramski et al. 2004). Moreover, a recent study found up to 60% of bulk particle backscattering in the ocean is contributed by submicron particles <0.7 μm with particles <0.2 μm (i.e. viruses and dissolved organic matter) contributing up to 40% of the bulk particle scattering (Zhang et al. 2020). With

this information, we can reduce the missing backscatter contribution to 20% of the total backscatter, with particles between 0.2 - 0.7 μm also contributing 20% of the total backscatter. With such a large contribution (~40%) of the <0.2 μm particles, this forces the question of how much viruses contribute to the dissolved fraction of the missing backscatter?

1.3 Backscatter by Viruses

Only one previous study has measured the backscatter by viruses. Balch et al. (2000) measured the light scattering of four bacteriophage cultures including human pathogens MS-2 (capsid size 25-30 nm) and T-4 (capsid size 100 nm), and marine phages Y-1 (capsid size 50-80 nm) and C-2 (capsid size 110 nm). The cultures in this experiment were isolated using an enrichment technique. This includes obtaining a pure host culture to be incubated with viral suspensions to promote virus proliferation. These enriched cultures were then filtered through a 0.22 μm filter to remove bacterial debris and then applied onto a lawn of the original host cell and observed for virus plaques. The isolated, purified page stocks were then subjected to ultracentrifugation to remove lysates and concentrate virus stocks. These phage stocks were then used in the optical experiments.

The light scattering properties of the viruses in this experiment were measured at concentrations of $10^{10} – 10^{12}$ mL^{-1}, which is 3-5 magnitudes higher than the concentration of viruses in surface seawater. Balch et al (2000) found that viruses in culture represent "0.2 to 2% of the total backscattering", but as a whole do not represent a major source of backscattered light (Balch et al. 2000).

However, Balch et al. (2000) only considered the contribution of viruses to total backscatter, not their contribution to the backscatter of the dissolved fraction. Furthermore, this conclusion was limited to bacteriophages with complex morphology (typically T4: 'head and tail' morphology) that are typically sized 30-100 nm. In the natural environment, marine viruses exist in a range of morphologies, and sizes (average size range of 20-300 nm) (Wommack and Colwell 2000; Suttle 2007). Most viruses that exist in the marine environment have a helical or icosahedral shape, with varying tail lengths or appendages (Balch et al. 2000), and their capsids vary in size, ranging from <30 nm - 750 nm (Bratbak et al. 1992). Due to the size and morphological variability of marine viruses in the natural environment, there is still significant uncertainty regarding the backscattering by viruses and their contribution to the 'missing backscatter'.

Now the question of how much viruses contribute to the missing backscatter is still open. Measurements on the backscatter of viral particles in the dissolved (<0.2 μm) fraction of seawater would provide evidence of their potential to impact backscatter measurements of seawater.

CHAPTER II – OBJECTIVES/HYPOTHESIS

2.1 Hypothesis

The goal of this MSc thesis project was to investigate the fractional contribution of viral particles to the optical backscatter of the dissolved fraction (<0.2 μm) of seawater. The underlying hypothesis is that the backscatter of the dissolved (<0.2 μm) fraction is directly proportional to virus concentration.

2.2 Objectives

The specific research objective is to conduct field and lab experiments to quantify the contribution of viruses to the backscatter in the dissolved fraction and to determine if, and to what extent marine viruses contribute to the missing backscatter in natural seawater. If successful, further characterization of optical backscatter could be used to extend the use of remote sensing by the potential development of satellite algorithms that quantify virus abundance and a method to study large-scale dynamics of viruses in the ocean.

CHAPTER III - METHODS

3.1 Sample Collection and Site

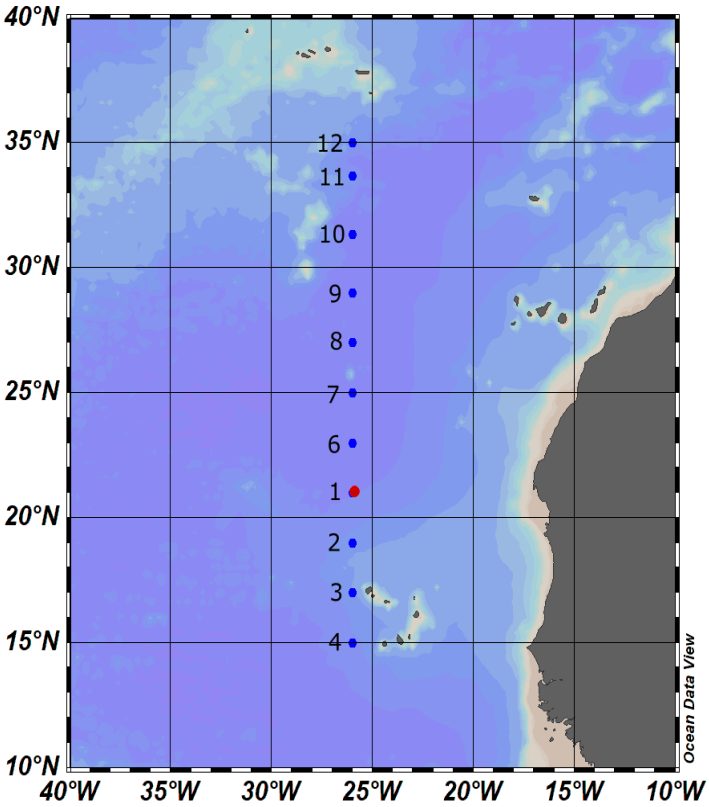

Figure 3.1 *STRATIPHYT-21 Cruise Transect*

Bathymetric map of the stations sampled during the STRATIPHYT-21 cruise transect in the Northeast Atlantic Ocean. Figure was prepared using Ocean Data View (ODV version 5.4.0).

Seawater samples and whole water (80 L) were collected from 12 stations during the early spring (February-March) of 2021 in the Northeast Atlantic Ocean during the STRATIPHYT-21 research cruise, which took place onboard the R/V Pelagia. The latitudinal transect spanned from 15°N to 35°N at ~ 26°W (Table A.1; Figure 3.1). Water samples were collected from a minimum of two depths within the euphotic zone (upper

200 m) using a rosette containing 24 polypropylene bottles (11.2 L each and manufactured by NMF-NIOZ) equipped with CTD (Seabird 9+) with standard sensors.

3.2 Fractionation Experiments

At each station, seawater samples were collected from a minimum of two depths within the euphotic zone. Each station had 1-2 shallow samples (<20 m) and 1-2 deep samples (>20 m). To elucidate the contribution of viral particles to optical backscatter in the dissolved fraction (<0.2 µm) of seawater, samples were subjected to size fractionation. Specifically, the samples were filtered through a Sterivex 0.2 µm filter onboard and stored at 15°C until transport. Once removed from the ship, transportation issues occurred related to COVID-19 and the seawater samples were held in non-ideal conditions (dark, room temperature environment) for ~6 months before transporting to the home lab. Bacteria likely proliferated in the samples during this time. In the home lab, the samples were further fractionated by a tangential flow filter (TFF) filtration (Vivaflow 50) using a 30 kDa molecular weight cutoff (MWCO) pore size PES-membrane. Ultrafiltrate (30 kDa filtrate) was obtained by recirculating each 0.2 µm filtrate sample over the cartridge filter with a discharge rate of 40 mL min^{-1}. To investigate the influence of viral particles on the backscatter of the dissolved fraction of seawater, two parameters were measured: viral abundance, and particulate backscattering coefficient (βbp).

3.3 Virus and Bacteria Abundance

Water samples (1 mL) were fixed in 2 mL cryovials for virus bacteria enumeration using 25% EM (electron microscopy) grade glutaraldehyde at a final concentration of 0.5% for 30 minutes at 4°C, flash frozen in liquid nitrogen and stored at -80°C until analysis. Virus and bacteria were enumerated from fixed samples using a Becton-Dickson FASC Celestra flow cytometer (FCM) measured using a 488 nm argon blue green violet (BGV) laser and Milli-Q water (18 megaohms [MΩ]) as sheath fluid.

For virus enumeration, thawed samples were diluted in TE buffer (pH 8.2, 10 mM Tris HCl, 1 mM EDTA), and stained with the nucleic acid-specific green fluorescence dye SYBR Green I at a final concentration of 0.5×10^{-4} and heated at 80°C for 10 minutes in the dark due to light sensitivity. The discriminator was set on green fluorescence, with the threshold set to 250. Blanks (TE Buffer and SYBR Green I) were treated the same way. Once cooled, the samples were analyzed for 1 min at a medium flow rate (~50 µL min^{-1}).

For bacteria enumeration, the protocol followed Marie's procedure (Marie et al. 1997, 1999). Thawed samples were diluted in TE buffer and stained with an SYBR Green I nucleic acid gel stain (final concentration of 1×10^{-4} of the commercial stock solution), then incubated in the dark at room temperature for 15 minutes. The discriminator was set on green fluorescence, with the threshold set to 1300. Once cooled, the samples were analyzed for 1 min at a medium flow rate (~50 µL min^{-1}).

The listmode files (FCM data files) were analyzed using FlowJo software (version 10.8.1). Viral and bacterial abundances were exported into an EXCEL file where viral abundances were corrected for blanks and viral and bacterial concentrations were

calculated based on time sampled, dilution, and flow rate. The change in viral and bacterial abundance between fractions (i.e., dissolved [<0.2 µm] - ULMW DOM [<30 kDa]) represent the viral particles that were removed during filtration in the North Atlantic samples (14 ± 21% recurring; 86 ± 21% removed). These measured abundances were compared to the particulate backscattering coefficient (βbp) to see a relationship between changes in viral abundance and the backscattering coefficient.

3.4 Microscopy

As a result of the non-ideal bottle storage, the 0.2 µm fraction samples were contaminated with bacteria, so the scattering measurements needed to be corrected to remove the influence of the bacteria. To estimate the size and concentration of bacteria required to model the contribution of bacteria to βbp in contaminated samples, fluorescence microscopy was used. The Olympus BX51 Fluorescence Microscope equipped with a 100W Hg lamp was used under blue excitation. Whole water from the North Atlantic (15 mL) was filtered through a 0.45 µm polycarbonate filter to remove phytoplankton and larger-sized organisms, and fixed with 1.5 mL of 10% glutaraldehyde for 7 minutes. After fixing, the filtrate was filtered onto a 0.2 µm pore-size 25mm black polycarbonate filter. The filter was then stained with SYBR Green I working solution (10%) for two minutes in the dark. For analysis, ~10 pictures were captured through the microscope, and the software ImageJ was used to measure the approximate average area (0.32 μm^2) and concentration (3.51×10^4 mL^{-1}) of bacteria in samples.

3.5 Backscatter

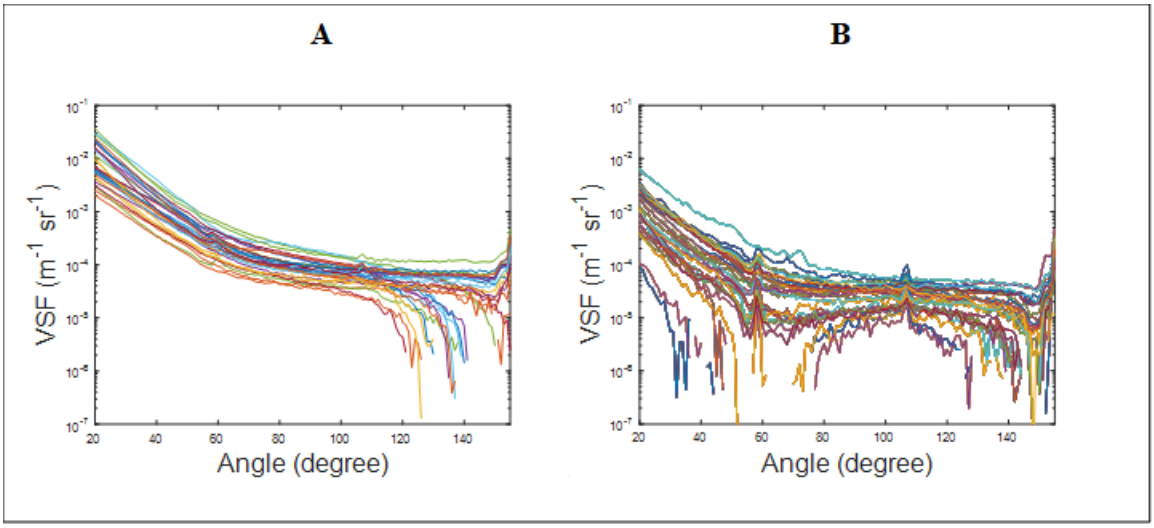

Figure 3.2 *VSFv of all dissolved and ULMW DOM samples*

A semilog plot (y-axis has a base-10 logarithmic scale) of all the VSFs of the dissolved **(A)** and ULMW DOM **(B)** samples from the STRATIPHYT-21 cruise. All samples visually look like the same shape in the dissolved samples, but vary in the ULMW DOM samples. Data <60° and >110° is not considered usable and are discarded. Angles from 60-110° are considered good data and consistent and will be used to measure the particulate backscattering coefficient. The figure panel was prepared using MATLAB (version 2019a).

To compare the optical properties of the dissolved and ULMW DOM (<30 kDa) fraction volume scattering properties were measured. The volume scattering function, the light scattering of a volume of matter, (VSF, $\beta(\Theta)$; m^{-1} sr^{-1}) was measured using a LISST-VSF (Sequoia Scientific, serial number 1664) equipped with a 517 nm laser. The LISST-VSF comprises two optical units, a laser diffraction unit (LISST) that measured the scattering from 0.08° to 14.4° at 32 angles and a "roving eyeball" unit that measured linearly polarized scattering from 15° to 155° with 1° increment. For every sample, each angle had 30 repeated angular measurements. Briefly, 1.5 L of each sample was poured gently to fill the holding chamber of the LISST-VSF to prevent bubbles from developing

that can interfere with measurements. Measurements were conducted in the dark to prevent light interference. All VSFs (dissolved and ULMW DOM) were viewed and analyzed using MATLAB over all angles, where the dissolved samples consisted of similar shapes (figure 3.2).

FCM rendered results were contaminated with bacteria, so correction methods here were applied to the data. To correct the bacteria, a combination of microscopy (Sec. 3.8), flow cytometry, and modeling was used. The bacteria's area and concentration that were measured by epifluorescence microscopy were used to model the contribution of the VSF for bacteria (VSF_b). The size distribution of bacteria from the North Atlantic whole water microscopy samples was used to calculate the bacteria VSF using Mie scattering theory, assuming that all the bacteria are spheres and the refractive index of all bacteria is 1.05.

Once the VSF_b was modeled, the correction was applied to all samples contaminated by bacteria. First, the ratio of the bacteria concentration found with FCM and microscopy ($\alpha\{i\}$) was calculated for the bacteria in each of the samples (Eq. 1).

(1)

$$(\alpha\{i\} = \frac{FCM\ bacteria\ concentration\left(\frac{N}{mL}\right)\{i\}}{average\ bacteria\ in\ microscopy\left(\frac{N}{mL}\right)\{whole\ water\}})$$

Then, to calculate the VSF of the dissolved fraction with bacteria correction ($VSF_{D\ corrected}$), the product of α and VSF_b was subtracted by the $VSF_{Dissolved}$ (Eq. 2). The VSFs of the corrected data are displayed in figure 3.3. Angles 90-110° are considered as 'good' as they show consistent shape and angles > 110° are considered poor quality data. Poor quality

data is a result of these particles being around the detection limit (around 10^{-5} m^{-1} sr^{-1}) of the instrument, and; therefore, have noisy results due to correcting the total scattering for the scattering of pure seawater. Then, the virus VSF value (VSF_{Virus}) of the V_f fraction was calculated, which is classified as the true virus scattering (Eq. 3).

(2)

$$\left(VSF_{D\ corrected} = VSF_{Dissolved} - (VSF_b \times \alpha)\right)$$

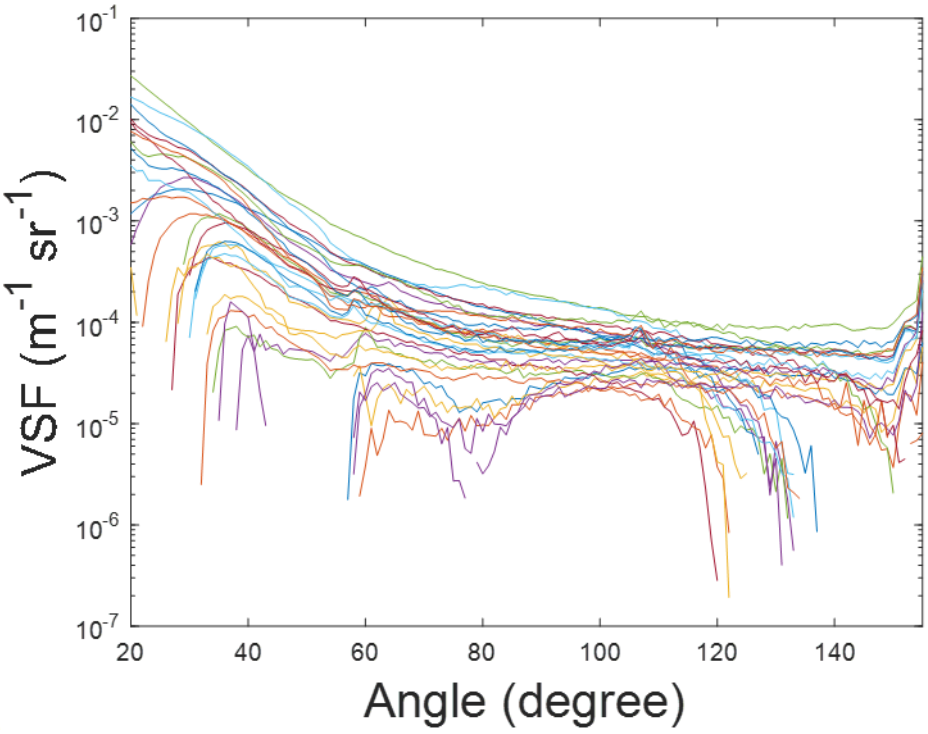

Figure 3.3 *VSFs of all corrected dissolved samples*

A semilog plot (y-axis has a base-10 logarithmic scale) of all the VSFs of the corrected dissolved samples. All samples visually look like the same shape from angles 90-115°. The figure panel was prepared using MATLAB (version 2019a).

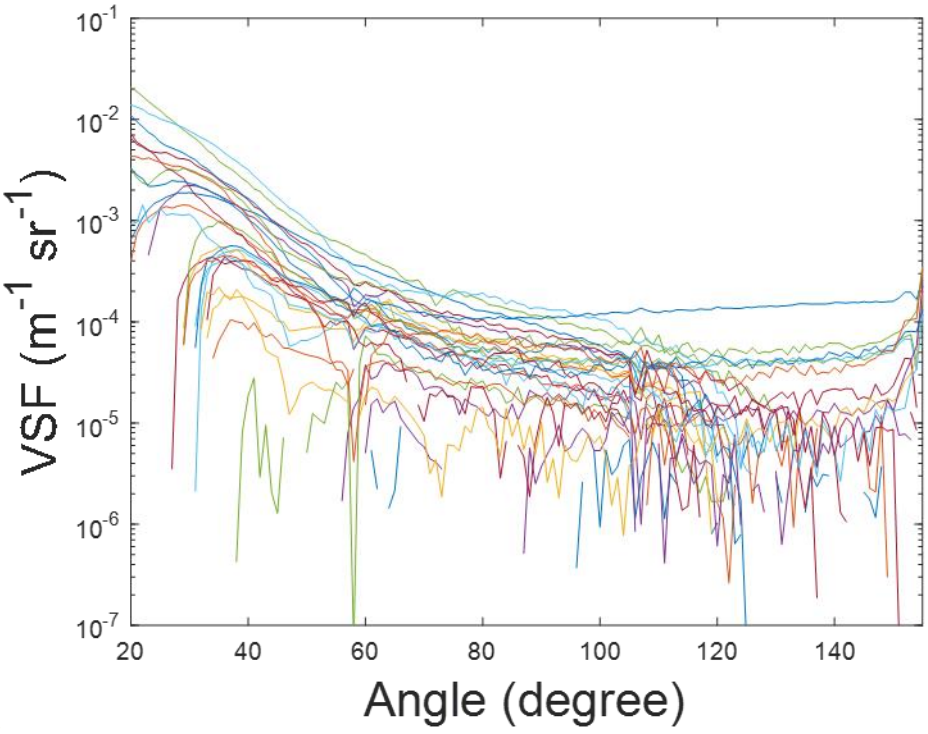

Figure 3.4 *All VSF_{Virus}*

A semilog plot (y-axis has a base-10 logarithmic scale) of all the VSFs of the virus fraction (VSF_{Virus}). The figure panel was prepared using MATLAB (version 2019a).

(3)

$$(VSF_{Virus} = VSF_{D\ corrected} - VSF_{ULMW\ DOM})$$

After correction was applied and VSF_{Virus} was measured (figure 3.4), interpolation of VSFs was needed due to holes in the VSF, which mean negative numbers as a result of the $VSF_{ULMW\ DOM}$ being higher than the $VSF_{D\ Corrected}$ in random areas, which can manipulate the data. Interpolation was conducted by using a moving median with a window

length of 50 to fill in the missing VSF_{Virus} VSFs. Figure 3.5 shows a visual representation of the processing of the VSFs.

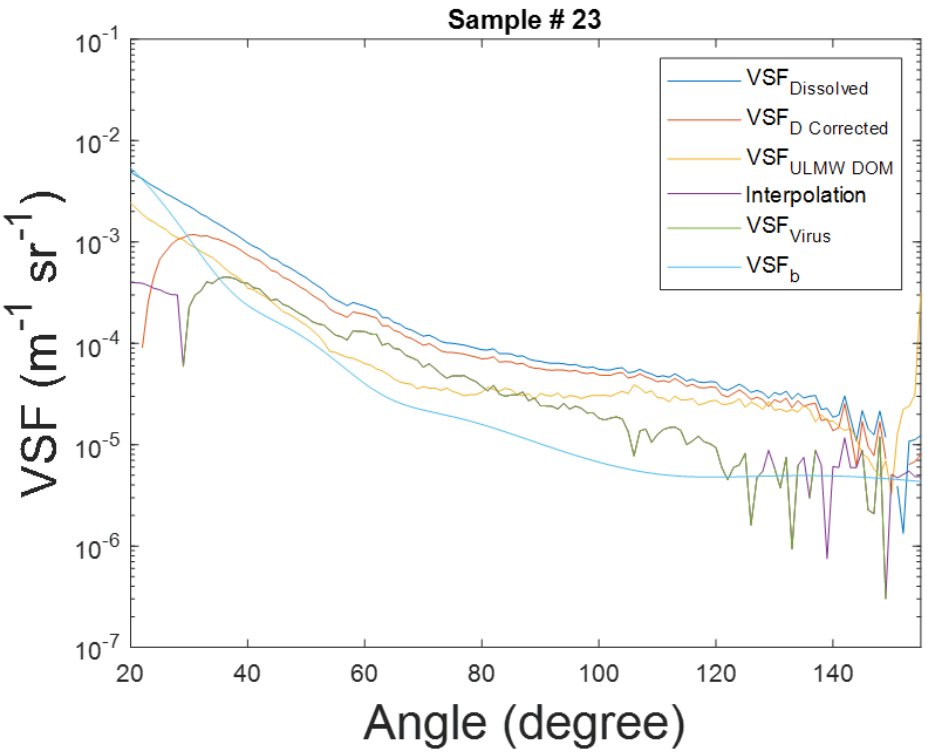

Figure 3.5 *Processing of VSFs*

A semilog plot (y-axis has a base-10 logarithmic scale) of an example of one individual sample VSF changes with fractionation and correction. The dark blue line represents the VSF of the dissolved sample, before the correction of bacteria. The red line indicates the VSF of the dissolved samples, corrected with bacteria. The yellow line represents the VSF of the ULMW DOM sample. The green line represents the original data of the virus fraction VSF and the purple segments indicate the filled-in missing data (negative data). The light blue line represents the modeled bacteria VSF. The interpolation was conducted on all samples. The figure panel was prepared using MATLAB (version 2019a).

The influence that viral-sized particles had on backscatter was determined by comparing the particulate backscattering coefficient between filtrates (dissolved and ULMW DOM). The average VSFs of the samples between angles 90-110° were used as a

proxy for the particulate backscattering coefficient ($\beta_{(100)}$). Angles >110° were scattered and classified as unusable data.

(4)

$$\beta_{(100)} = \frac{1}{n}\sum_{i=1}^{n} \beta(90 - 110)$$

Equation 4 was used to measure the backscattering of the three fractions ($VSF_{D\ Corrected}$, $VSF_{ULMW\ DOM,}$ and VSF_{Virus}) to calculate each fraction $\beta_{(100)}$ ($\beta_{Dissolved}$, $\beta_{ULMW\ DOM}$, and β_{Virus}, respectively). The percent backscatter viruses have in the dissolved fraction ($\%\beta_{Virus}$) is calculated with Eq. 5.

(5)

$$(\%\beta_{Virus} = (\frac{\beta_{Virus}}{\beta_{Dissolved}}) \times 100)$$

3.6 Statistical Analysis

All statistical analysis was conducted using MATLAB (version 2019a) and statistical tests included, one-way ANOVAs, T-tests, and regressions. One-way ANOVAs were performed between sample depths with latitude, and on the VSFs between fractions. T-tests were performed on the viral abundance, and β(100) values between filtrates and on bacteria abundance between FCM enumeration methods. Regression analyses were performed on the β_{Virus} values with depth and latitude, and a

comparison of virus backscatter and viral abundance. The significance (p-value < 0.05), if any, would provide information on the significance of the parameters in each fraction.

CHAPTER IV – RESULTS

4.1 Virus and Bacteria Abundance

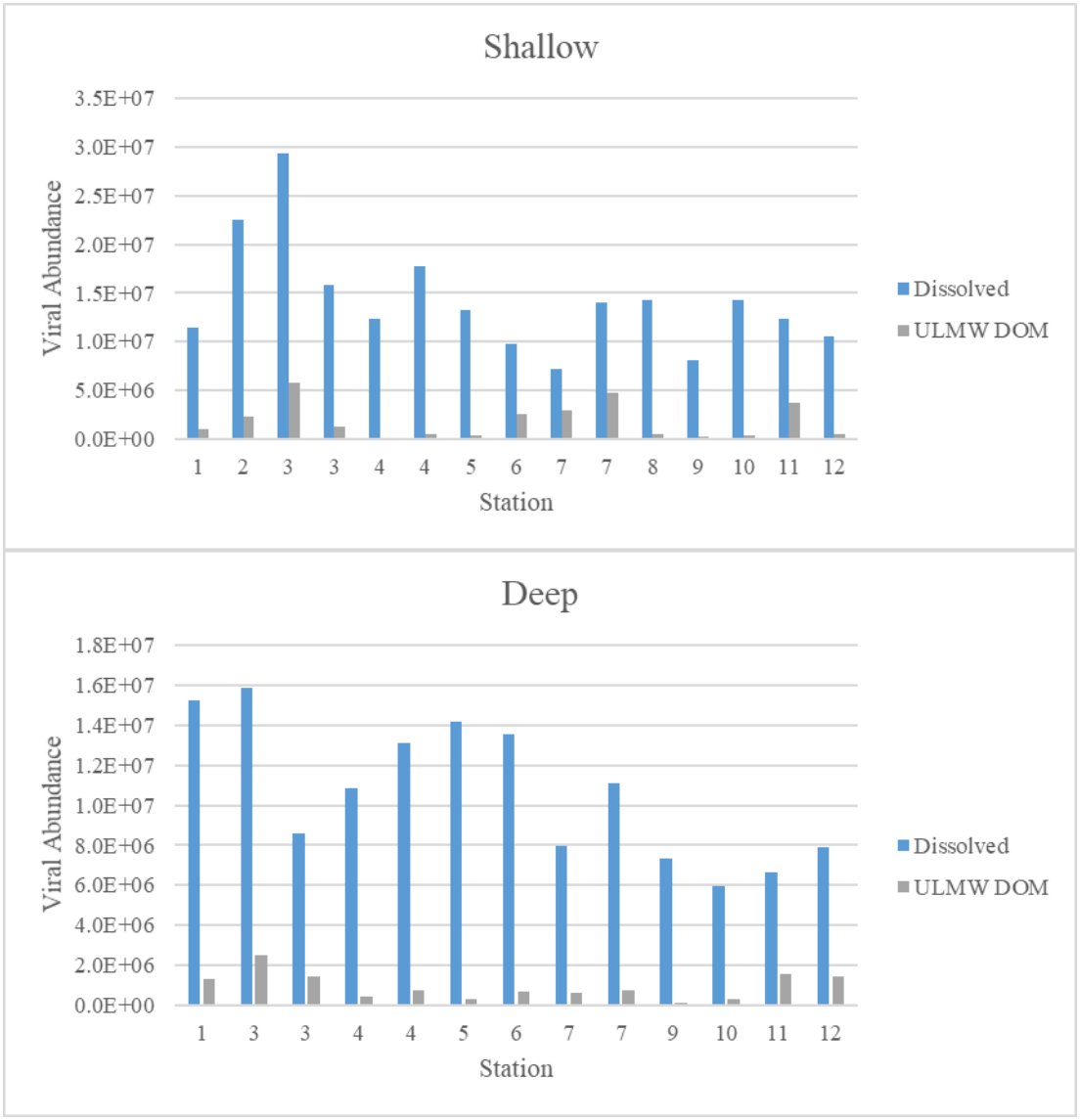

Figure 4.1 *Viral abundance of the dissolved and ULMW DOM fractions by stations*

A bar chart of the viral abundance (mL^{-1}) of the dissolved and ULMW DOM fractions in the shallow and deep samples by stations during the STRATIPHYT-21 North Atlantic research cruise. The viral abundance in the dissolved fraction are significantly higher than the viral abundance in the ULMW DOM fraction in the shallow and deep samples (t-test; p-value < 0.05). The data presented is quality-controlled data.

Virus abundance was measured in all samples of the dissolved (<0.2 μm) and ULMW DOM (<30 kDa) fractions. Overall, there were five distinct virus populations present in the dissolved samples consisting of bacteriophages (V1, V2, V3) in all of the samples and algal viruses (V4, V5) in seven of the samples, which are larger viruses determined based on their high side scatter values (Castberg et al. 2001). The expectation is that the 30 kDa ultrafiltration would remove viruses, resulting in a higher viral abundance in the dissolved fraction and a reduced abundance in the ULMW DOM fraction (figure 4.1). Indeed, the viral abundance in the dissolved fraction was significantly higher than in the ULMW DOM fraction in both shallow and deep samples (t-test; p-value < 0.05). However, the FCM analysis revealed that contrary to our expectations, some viruses were still present in the ULMW DOM samples. One sample was considered an outlier as it contained a higher number of viruses in the ULMW DOM fraction than the dissolved fraction and, as this violates the assumption of the methodology, it was removed from the analysis. Ultrafiltrate, on average, reduced viral abundance by 90.1 ± 9.3%. In Figure A.1, cytograms are presented using FlowJo software that shows distinct V1, V2, V3, and V4 in the dissolved fraction, where most viruses were removed in the ULMW DOM sample.

Problems arose when processing the FCM data as bacteria contaminated the dissolved fraction. Bacterial contamination was present in all of the dissolved samples, which lead to additional correction methodology by using microscopy and modeling, as explained above in Sec. 3.5. Ultrafiltrate, on average, reduced bacteria abundance by 92.2 ± 10.1%. Figure A.1 contains cytograms presented using FlowJo software that shows

distinct bacterial contamination in the dissolved fraction, where most bacteria were removed in the ULMW DOM sample.

After bacteria were discovered while processing the FCM data, the influence of the staining protocol on enumerating bacteria in virus samples was then conducted. There are two separate staining protocols for bacteria and viruses. To ensure that bacteria counts were accurate (after being counted using the virus staining protocol); both methods were tested for comparison. Figure A.2 shows the cytograph that shows the bacteria abundance with each staining method (virus enumeration and bacteria enumeration). The two methods showed that there was a significantly higher yield of bacteria when the samples were stained using the virus protocol (average concentration of $3.81 \times 10^5 \pm 1.22 \times 10^4$ mL^{-1}) compared to the bacteria protocol (average concentration of $3.48 \times 10^5 \pm 6.21 \times 10^3$ mL^{-1}) (t-test; p-value < 0.05). Since the samples were prepared using the virus staining method, the results represent an overestimation of bacteria rather than an underestimation. Therefore, no adjustment of the correction for bacteria counts was necessary based on potential staining discrepancies between the two staining protocols.

4.2 Backscatter

The $\beta_{(100)}$ that was used as a proxy for the particulate backscattering coefficient was measured in the dissolved and ULMW DOM fractions with the expectation being that the difference between the $\beta_{(100)}$ in the two fractions would largely reflect the backscatter contribution by viruses. The limitation of this assumption is that there is a possibility that dissolved particles (organic or inorganic), other than viruses, that are also present in the >30 kDa fraction contribute to the backscatter. In Figure 4.2, the $\beta_{(100)}$ of the dissolved and

ULMW DOM filtrates is examined across all samples. As expected, most samples had a higher $\beta_{Dissolved}$ than the $\beta_{ULMW\ DOM}$. Four samples (samples 2, 3, and 25) had a higher $\beta_{ULMW\ DOM}$ than the sample's respective $\beta_{Dissolved}$, resulting in a negative β_{Virus} (virus particulate backscattering). One sample (sample 22) had a negative backscatter in the ULMW DOM fraction. These samples (totaling four samples) are defined as poor-quality data and removed from the analysis. Moreover, there was a significant difference in the $\beta_{(100)}$ between dissolved and ULMW DOM fractions in different depth layers, whereas $\beta_{Dissolved}$ was significantly higher than $\beta_{ULMW\ DOM}$ in both the shallow and deep samples (t-test; p-value < 0.05).

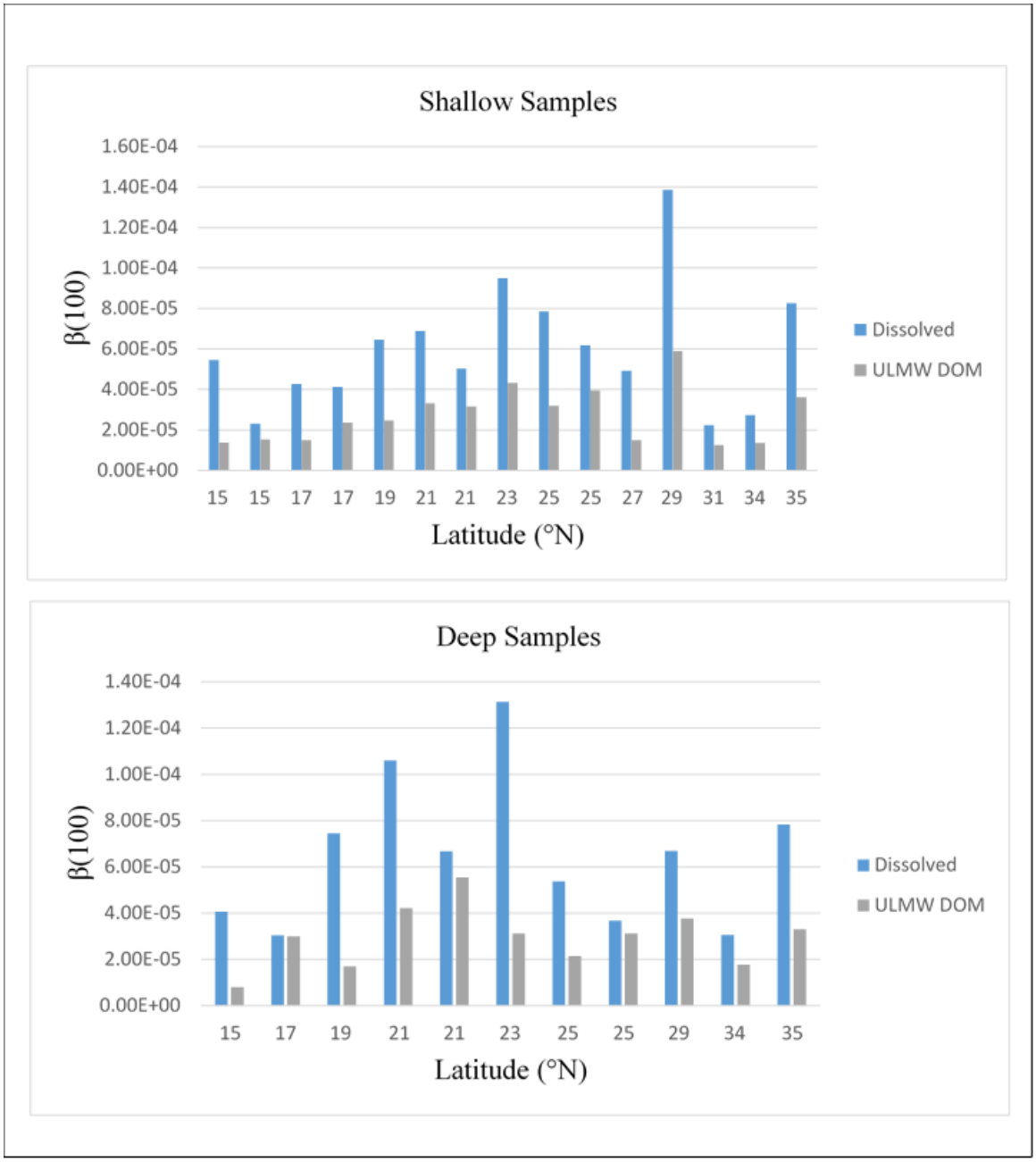

Figure 4.2 *Backscatter of the dissolved and ULMW DOM fractions with latitude*

A bar chart of the backscattering (β_{100}) values of the dissolved and ULMW DOM fractions in the shallow and deep samples by latitude during the STRATIPHYT-21 North Atlantic research cruise. The backscatter in the shallow samples are significantly higher than the backscatter in the deep samples (t-test; p-value < 0.05). The data presented is quality-controlled data.

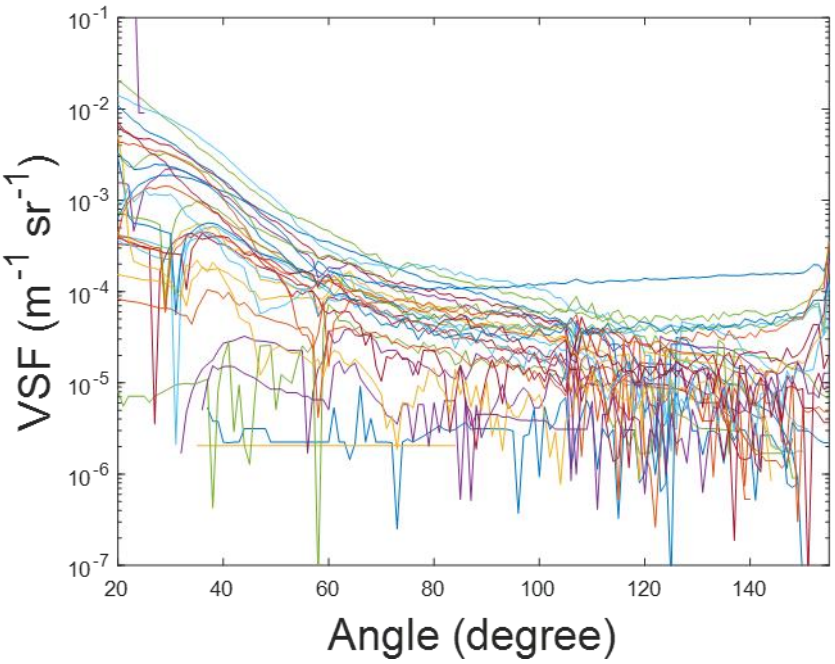

Figure 4.3 *All interpolated VSF_{Virus}*

A semilog plot (y-axis has a base-10 logarithmic scale) of all the interpolated VSFs of the virus fraction. The figure panel was prepared using MATLAB (version 2019a).

Figure 4.3 displays the interpolated VSFs of the virus fraction (VSF_{Virus}). The VSF_{Virus} is used to calculate the β_{Virus}, shown in figure 4.4 with depth and latitude, where the negative samples (samples 2, 3, and 25) violated the assumption of the method (that ultrafiltration removes viruses) and, therefore, removed during data quality control as deemed poor quality data. A one-way ANOVA test was conducted on the shallow and deep samples. This showed that the β_{Virus} between the sample depths was not statistically significantly different (one-way ANOVA; p-value > 0.05). A regression analysis was then applied to data within each depth layer as a function of latitude. For the shallow samples, there was a non-significantly positive relationship with latitude (linear regression analysis; R = 0.2187, R^2 = 0.0478, p-value > 0.05).

For the deep samples, there was a non-significantly negative relationship with latitude (linear regression analysis; R = -0.2329, R^2 = 0.0542, p-value > 0.05). A linear regression analysis was conducted on the β_{Virus} with latitude. This revealed that β_{Virus} had a non-significant negative relationship with latitude (linear regression analysis; R = -0.0531; R^2 = 0.00282; p-value > 0.05).

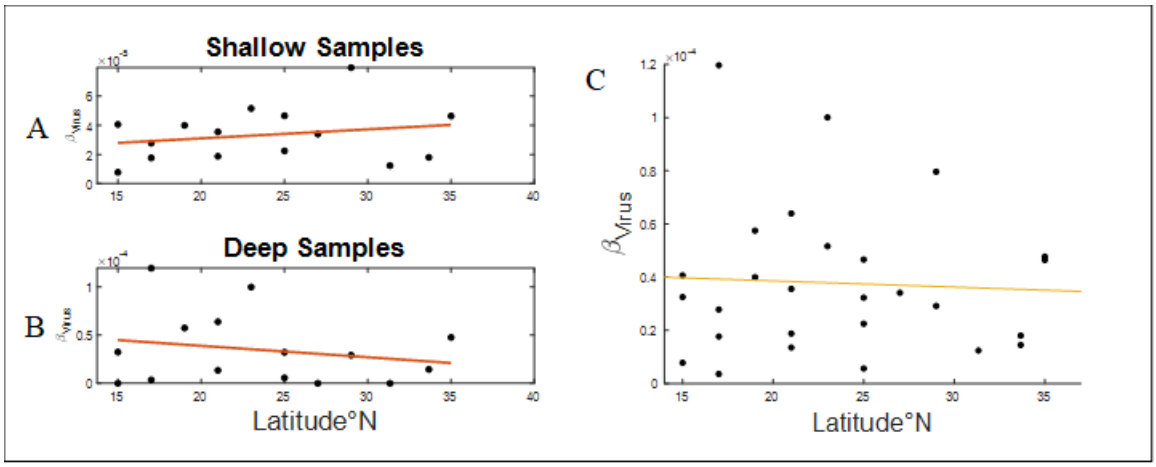

Figure 4.4 *Virus Backscatter (β_{Virus})*

Scatter plots of β_{Virus} (virus backscattering) with depth and latitude during the STRATIPHYT-21 North Atlantic research cruise. The black dots indicate the data points and the yellow and orange lines show the linear relationships. The β_{Virus} between the fractions in the shallow (A) and deep (B) samples are not statistically significantly different (p-value > 0.05) and there was a non-significantly negative relationship with latitude (C) (linear regression analysis; R = -0.0531; R2 = 0.00282; p-value > 0.05). Scatter plots were prepared using MATLAB (version R2019a).

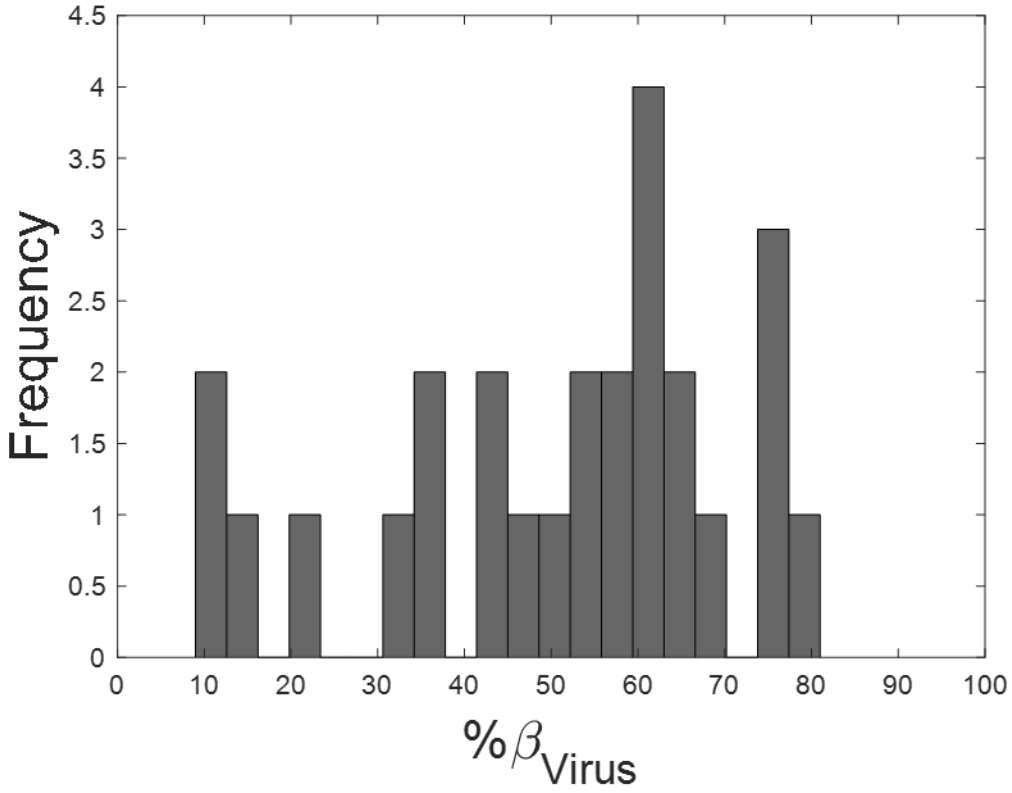

Figure 4.5 *%β_{Virus} distribution*

A histogram of the distribution of the percent contribution viruses have in the dissolved particulate backscattering. The percent contribution viruses have in the dissolved fraction varies. The highest frequency of the four samples has between 59-63%. The figure panel was prepared using MATLAB (version 2019a).

The %β_{Virus} was used to show the contribution of viruses to the optical backscatter in the dissolved fraction. The percent contribution by viruses in the dissolved fraction ranged from 10-80% (Figure 4.5) with the highest frequency of 59-63%. It was assumed the %β_{Virus} would be directly influenced by the percent contribution of viruses removed from the dissolved fraction. One sample was considered an outlier of the percent viruses removed and was removed from the analysis.

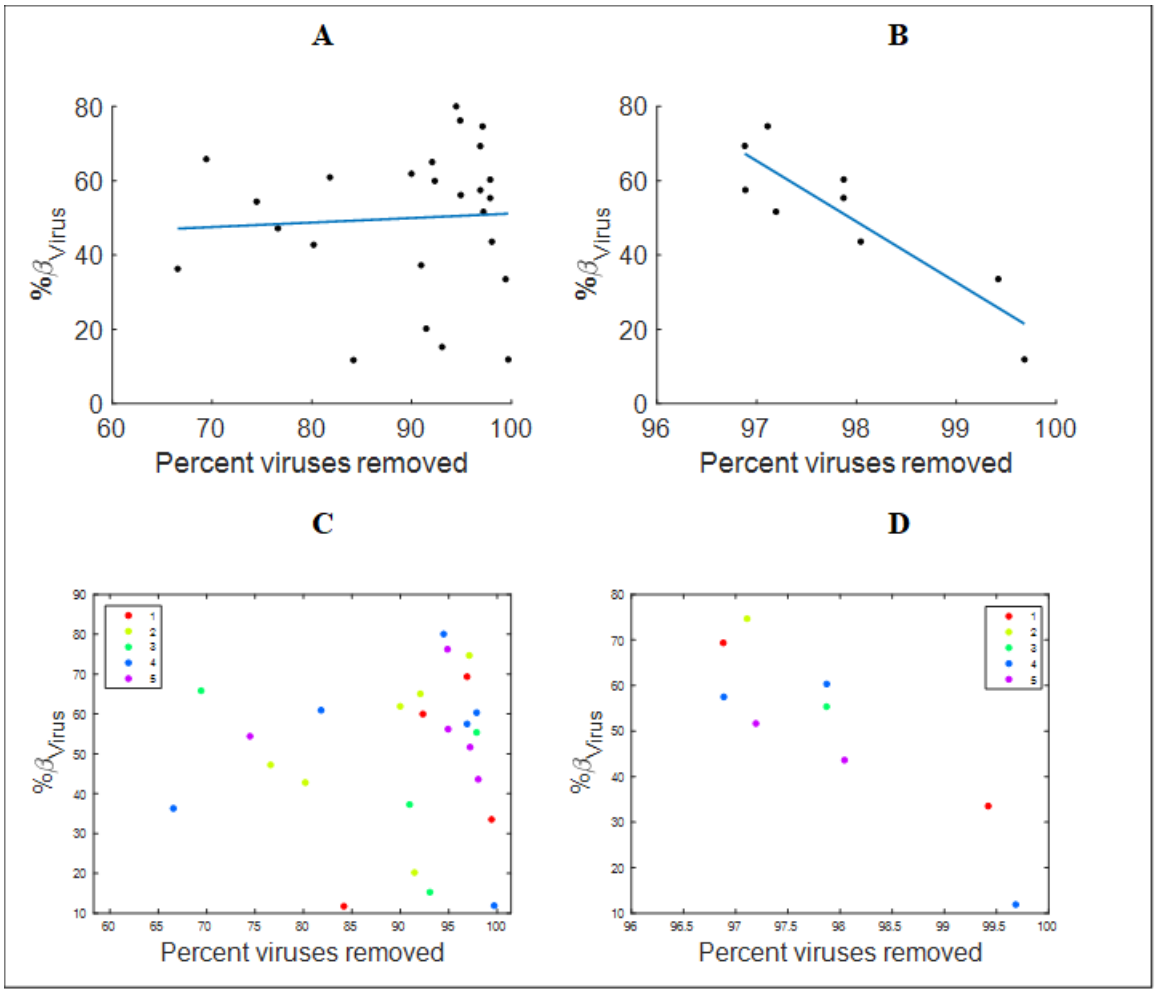

Figure 4.6 *%β_{Virus} relationship to viruses removed*

Scatter plots of %β_{Virus} (percent contribution of virus backscattering to the dissolved fraction) with percent viruses removed and depth during the STRATIPHYT-21 North Atlantic research cruise. The black dots indicate the data points and the blue lines show the linear relationships. The %β_{Virus} with all data points is non-significant positive relationship (linear regression analysis: R = -0.0594, R2 = -0.0398, p-value > 0.05) (A). The highest quality data of %β_{Virus}, there is a significantly negative relationship (linear regression analysis: R = -0.89, R2 = 0.792, p-value < 0.05) (B). When considering this relationship with use of filters, there is no clear relationship with the use of filters (C). When looking at the highest quality data (D), the plots range in number of filter usages. Scatter plots were prepared using MATLAB (version R2019a).

As a result, a positive relationship between the %β_{Virus} and the percent viruses removed was expected due to the assumption that more viruses would equate to a higher

$\%\beta_{Virus}$. However, figure 4.6 shows that the $\%\beta_{Virus}$ relationship to viruses removed is a non-significant positive relationship (linear regression analysis: $R = -0.0594$, $R^2 = -0.0398$, p-value > 0.05). However, when only concentrating on the highest quality data of viruses removed (96-100%), there is a significantly negative relationship (linear regression analysis: $R = -0.89$, $R^2 = 0.792$, p-value < 0.05). When examining the relationship between $\%\beta_{Virus}$ and percent virus removal to filtration (figure 4.6 C and D), there is no clear relationship between the number of times the filters were used to the results between these two parameters.

Flow cytometric analysis revealed the presence of bacteria in the dissolved fraction samples. Accordingly, backscatter measurements were corrected to remove the contamination of bacteria. To ensure that corrections did not affect the overall trends in the data, statistical analysis was performed to compare uncorrected and corrected data. The uncorrected and corrected data were not statistically significantly different (one-way ANOVA; p-value > 0.05). The dissolved fraction was corrected by 24.3 ± 13.6%. Since these analyses have revealed the same trends as before the correction, the corrected values and analyses are appropriate to use.

4.3 GOM Case Study

To verify that the results from the NA were not significantly affected by (1) non-ideal storage of samples and (2) bacterial contamination of dissolved fraction, analysis was repeated in three seawater samples from the GOM in the Mississippi Bight (Petit Bois, Horn Island, and Cat Island or locations A, B, and C, respectively) (figure 4.7).

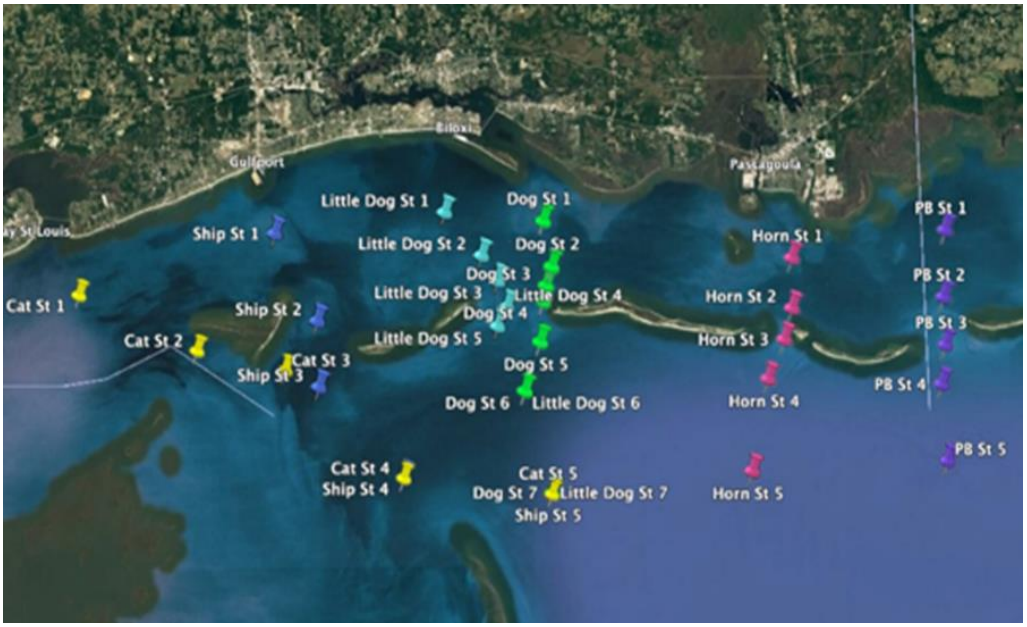

Figure 4.7 *GOM sample locations*

A map of the stations sampled during in the Gulf of Mexico. Locations Petit Bois, Horn Island, and Cat Island are labelled sites A, B and C, respectively.

4.3.1 Virus and Bacteria Abundance

The virus and bacteria counts were measured to see if bacteria abundance increased with time. It was expected to have an increased abundance of bacteria in the sample compared to what was measured in the samples before being stored. Then after the sample was filtered again, the bacteria were expected to be removed. In all samples, a considerable amount of bacteria was present after non-ideal storage. Then after the samples were filtered through a 0.2 µm filter again, the bacteria were no longer in the sample (Figure A.3). On average, bacteria abundance increased by 446% after being stored in non-ideal conditions and filtration removed 86 ± 17% of bacteria in the samples.

Overall, there were three distinct virus populations present in the dissolved samples consisting of bacteriophages (V1, V2, and V3). One sample was removed from

the analysis as it contained a higher number of viruses in the ULMW DOM fraction than in the dissolved fraction. Ultrafiltrate, on average, reduced viral abundance by 98.7 ± 1.3%. Since the VSF is variable with the concentration and size of particles in the sample, the backscatter is affected by bacteria contamination in the samples. The backscatter is suspected to increase after being held in non-ideal conditions because of bacteria growth, then decrease after the bacteria have been removed, and decrease once again after viruses are removed.

4.3.2 Backscatter

The VSF was measured to relate the flow cytometry abundance of bacteria and viruses to the backscatter and to see if the backscatter was influenced by the changes in bacteria and virus abundance. It was expected to see a difference in the backscatter since there was a significant difference in bacteria and virus abundance between filtrations. The data showed that there was a significant difference in the VSF (from angles 90-110°) between the different fractions (outlined in table 4.1) (one-way ANOVA; p-value < 0.05).

Fraction A is described as the ideal dissolved fraction sample and fraction E is the ideal 30 kDa fraction. The non-ideal dissolved fraction (B) is fraction A after non-ideal storage, where bacterial contamination was present, and fraction C is fraction B after additional 0.2 µm filtration, where bacterial contamination is removed, and lastly, fraction D is fraction C with 30 kDa filtration (non-ideal 30 kDa). Bacterial contamination can alter DOM concentration and composition, and viruses, so evaluating the changes in these fractions can show the bacteria changes between the ideal and non-ideal samples.

Table 4.1 *GOM case study fractions*

Fractions	**Definition**	**Viral Abundance (mL^{-1}) (avg $x10^{+07}$ ± S.E)**	**Bacterial Abundance (mL^{-1}) (avg $x10^{+05}$ ± S.E)**
A	0.2 µm t_0	3.55 ± 1.31	5.70 ± 0.975
B	0.2 µm t_4	3.39 ± 0.365	25.9 ± 3.77
C	0.2 µm $t_{4+filtration}$	3.27 ± 1.75	2.74 ± 1.68
D	C + 30 kDa filtration	0.0227 ± 0.00589	0.0158 ± 0.00464
E	A + 30 kDa filtration	0.334 ± 0.263	0.482 ± 0.264
$VSF_{GOM\ B}$	Bacteria influence; B – C		23.4 ± 9.33
V_{fA}	Virus fraction with no influence of bacterial contamination; A - E	4.92 ± 0.994	
V_{fB}	Virus fraction with the influence of bacterial contamination; C - D	3.25 ± 1.76	

A table describing each sample fraction in the GOM case study. Fraction A is defined as the original dissolved fraction, filtered and measured within 24h of collection. Fraction B is measured after non-ideal storage for 4 months. Fraction C is measured after non-ideal storage that has been filtered through a 0.2 µm filter. Fraction D is measured after non-deal stored, 0.2 µm filtration, and then filtered through a 30 kDa filter. Fraction E is the original ULMW DOM fraction filtered and measured within 24h of collection. Bacterial VSF influence ($VSF_{GOM\ B}$) is measured by subtracting fractions B and C. The virus fractions (V_{fA} and V_{fB}) show viruses VSF contribution by subtraction of the dissolved and ULMW DOM fraction in the ideal and non-ideal conditions.

Figure 4.8 shows how bacteria growth and filtration affected the backscatter in the GOM samples. For the non-ideal conditions, it was expected to see a difference in the VSF between the varying fractions due to the increased abundance of bacteria and the

subsequent removal of bacterial and viral-sized particles. Indeed, the VSF decreases with filtration, as bacteria and viruses are removed. Specifically, the increased VSF in fraction B was from the increased abundance of bacteria in the sample. A decrease in VSF was observed after being filtered in the 0.2 µm fraction for a second time (C) after the bacteria were removed. The VSF decreased more in fraction D after virus-sized particles were removed.

The difference between the B and C fractions shows the bacteria's contribution to the VSF ($VSF_{GOM\ B}$; B – C). Since there is a considerable number of bacteria present, directly affecting the VSF measurement, this could lead to discrepancies in the 30 kDa fraction (D and E) from the possible contribution of DOM in the ULMW DOM fraction. Figure 4.8 (C) shows that the ideal 30 kDa fraction had a higher VSF than the non-ideal VSF. This suggests that with time, microbial processing did not introduce DOM in the ULMW DOM fraction. When looking at the virus abundance in these fractions, fraction E had, on average, 15 times higher virus concentration than fraction D. The higher virus abundance could be the cause for the higher ULMW DOM VSF.

For the ideal conditions (fractions A and E), it was expected the see a decreased VSF between the dissolved and ULMW DOM fraction due to the removal of viral-sized particles. As expected, the VSF decreases with size fractionation, which was expected because of viruses being removed. When comparing the virus fractions between the ideal (V_{fA}) and non-ideal (V_{fB}) samples, the backscatters (β_{vA} and β_{vB}) are not statistically significantly different (one-way ANOVA; p-value > 0.05). The virus abundance in these fractions was also not statistically different from one another, which can explain the

similar VSFs in these fractions as well (one-way ANOVA; p-value > 0.05). These results are consistent with all samples.

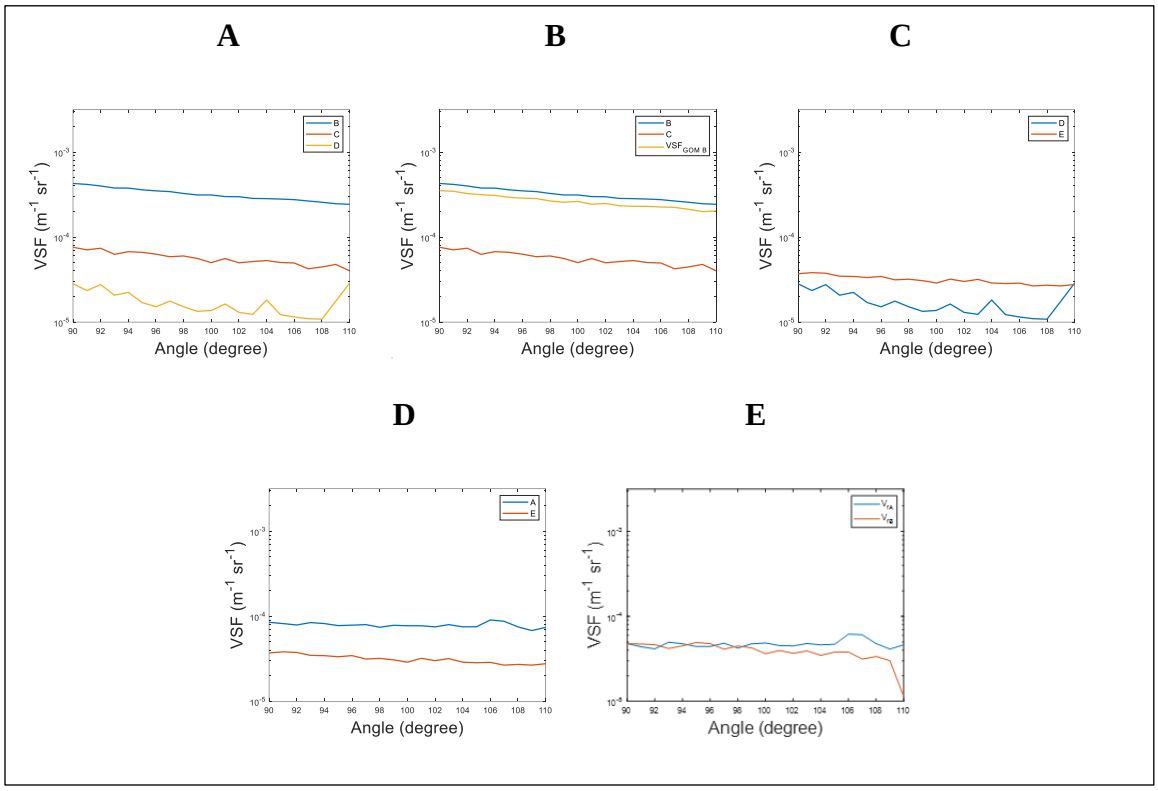

Figure 4.8 *Backscatter of GOM case study*

Semilog plots (y-axis has a base-10 logarithmic scale) of one samples VSF values in all of the GOM fractions (A, B, C, D, and E). Figure A displays the dissolved and ULMW DOM samples in non-ideal conditions. Figure B displays the bacteria's contribution to the VSF ($VSF_{GOM\ B}$) in the non-ideal sample. Figure C displays the microbial processing influence on the ULMW DOM fraction with time. Figure D shows the original ideal samples dissolved and ULMW DOM VSFs. Lastly, figure E displays the virus fractions between the ideal (V_{fA}) and non-ideal sample (V_{fB}), where the lines are closely related (visually). Visually, all the lines have different values. The VSF increases after being held in non-ideal conditions and then decreases with each filtration. Semilog plot was prepared using MATLAB (version R2019a).

The $\%\beta_{Virus}$ was used to show the contribution of viruses to the optical backscatter in the dissolved fraction. Table 4.2 lists the percent contributions of the GOM samples

(ideal, A, and non-ideal, B). Percentage contribution varied in both of the samples, averaging 36.5% for ideal conditions, and a higher average of 62.8% for non-ideal conditions. It is expected that the $\%\beta_{Virus}$ is directly positively influenced by the percent contribution of viruses removed in the dissolved fraction through filtration. However, figure 4.9 shows the $\%\beta_{Virus}$ relationship to viruses removed is a non-significant negative relationship (linear regression analysis: R = -0.7284, R^2 = 0.531, p-value > 0.05).

Table 4.2 *$\%\beta_{Virus}$ in GOM*

Sample Location	**Ideal $\%\beta_{Virus}$**	**Non-ideal $\%\beta_{Virus}$**
A	22.17%	71.96%
B	60.12%	69.23%
C	27.35%	47.12%

A table of the percent contribution viruses have in the dissolved particulate backscattering of the GOM samples (ideal and non-ideal). The ideal samples (A) have an average of 36.5% contribution and the non-ideal samples (B) have an average of 62.8% contribution. Percent contribution varied from 22-71%.

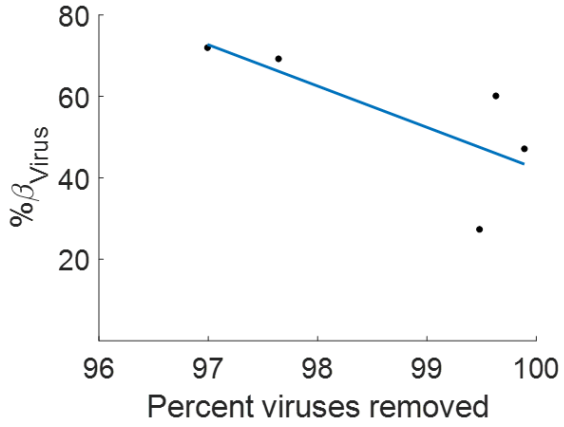

Figure 4.9 *GOM $\%\beta_{Virus}$ relationship to viruses removed*

Scatter plots of GOM $\%\beta_{Virus}$ (percent contribution of virus backscattering to the dissolved fraction) with percent viruses removed and depth during the GOM case study. The black dots indicate the data points and the blue line shows the linear relationships. There was a non-significantly negative relationship with the percent viruses removed (linear regression analysis: R = -0.7284, R2 = 0.531, p-value > 0.05). Scatter plots were prepared using MATLAB (version R2019a).

CHAPTER V – DISCUSSION

5.1 North Atlantic Experiment

The FCM and backscatter results have both revealed differences through size fractionation of seawater in the dissolved size range. Unfortunately, due to COVID-19-related delays in shipping, the samples were stored in non-ideal conditions (i.e. non-temperature controlled room for ~6 months) before transport to a home lab where they were placed. Ideal conditions include being stored in a dark, cool (4°C) environment and processing within 1 month of collection to prevent biological activity from changing water particle content. This has led to an increased bacterial abundance in the samples after original sampling and onboard filtration. Biological activity (i.e. bacteria growth and microbial processing of DOM) has the potential to change the initial IOP of seawater and thus interfere with the results presented here. Specifically, when looking at the dissolved (<0.2 µm) fraction backscatter data, the backscatter is contributed by viruses, DOM, and bacteria, instead of the proposed viruses and DOM.

Since a significant number of bacteria were present in the samples, a correction for the backscatter contributed by the bacteria needed to be applied to the backscatter data before considering the influence of viruses. The correction that was applied used a combination of microscopy, FCM, and Mie scattering modeling. Once the correction was applied, statistical analyses revealed that the relationships were unaltered, providing confidence that the correction had not influenced our results. After correction was applied, the results showed that filtration significantly decreased the backscattering between the dissolved and ULMW DOM fractions (t-test; p-value < 0.05). The difference in backscatter between these fractions revealed the backscatter that is contributed by

viral-sized particles. These particles' contribution to the dissolved backscatter ranged from 10-80% in the oligotrophic North Atlantic waters. The percent contribution viruses scattering has in the dissolved fraction ($\%\beta_{Virus}$) revealed that the percent contribution varies and possibly makes a significant contribution to dissolved backscattering that cannot be ignored.

When relating the $\%\beta_{Virus}$ to the highest quality data of the percent viruses removed, there was a significantly negative relationship. When examining the relationship between $\%\beta_{Virus}$ and percent virus removal with filter usage, there was no clear relationship, suggesting that filter efficiency was not related to the number of times the filter cartridge was used. Moreover, when only considering the highest quality data (>96% removal) no relationship was found to the number of times the filter was used, and instead is related to the efficiency of the filter. This negative of $\%\beta_{Virus}$ and percent virus removal does not fit our original expectation and may be due to the DOM and inorganic matter that is removed with filtration, contributing to the backscatter, which was not considered in the present study.

5.2 GOM Case Study

To further elucidate how bacterial contamination may have altered our results, the GOM case study was conducted in February 2022 by collecting 3 samples sampled from the furthest station in three different areas in the Mississippi Bight in the Gulf of Mexico (Petit Bois, Horn Island, and Cat Island). Once collected, samples were processed under ideal and non-ideal conditions to evaluate the potential changes in the VSF analyses.

In ideal conditions, the viral abundance decreased with ultrafiltration, having a direct influence on the VSF between the dissolved and ULMW DOM fractions. For the non-ideal conditions, the bacteria abundance increased by 443% after being held in non-ideal conditions for ~4 months. Once the bacterial contaminated filtrate was filtered through a 0.2 µm filter, the bacteria abundance decreased, leaving viruses present in the sample. Then with 30 kDa filtration, the viral abundance decreased.

The changes in bacterial and viral abundances revealed changes in the VSF (from angles 90-110°) between these fractions. The VSF was directly influenced by the bacterial and viral abundance, increasing as bacteria abundance increased and decreasing once bacteria and virus abundance decreased. This experiment shows that a change in bacteria and virus abundance affects the backscatter signal received from the varying fractions, signifying that these particles have a significant effect on the backscatter of seawater. In addition, this study can reveal the true VSF of the virus fraction (V_f) of seawater. The virus backscatter contribution to the dissolved backscatter ranged from 20-70% in the ideal and non-ideal storage Gulf of Mexico samples. The percent contribution viruses scattering has in the dissolved fraction ($\%\beta_{Virus}$) revealed that the percent contribution varies and possibly makes a significant contribution to dissolved backscattering.

The change in backscatter from the dissolved fraction after bacteria abundance increased and after being filtered again ($VSF_{GOM\ B}$, B - C), shows the contribution of bacterial cells to VSF, which has then compared to the modeled VSF from microscopy to justify if our correction methodology was valid (figure 5.1). The results rendered that the bacteria VSF from the GOM bacteria showed a higher VSF value than the one that was

modeled from the microscopy samples; however, the slope of the lines is identical (figure 5.1). There was a 1.81% relative uncertainty in prediction from angles 90-110, which is the angles that were examined in this current study. The slope is an indication of the bacteria's size. If the microscopy VSF is shifted upwards, the VSF from the GOM and microscopy are highly correlated and not significantly different (one-way ANOVA; p-value > 0.05). This gives us confidence that the methodology applied to correct backscatter data was valid.

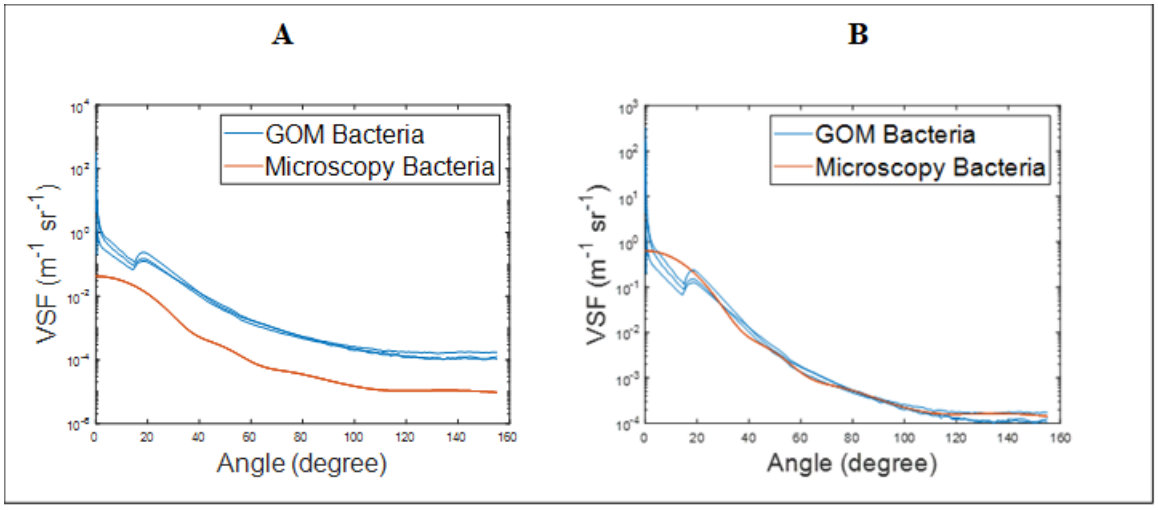

Figure 5.1 *Bacteria VSF comparison*

A semilog plot (y-axis has a base-10 logarithmic scale) that shows the VSF values in GOM bacteria fraction and modeled bacteria VSF from NA microscopy samples. The blue lines represents the VSFs of the bacteria fraction in the GOM case study. The orange line represents the VSF of the modeled bacteria from the NA microscopy. Visually, the lines slopes look similar, but the GOM bacteria is shifted upwards (A). When the microscopy VSF is shifted upwards (B), the lines are not significantly different (one-way ANOVA; p-value > 0.05). The semilog plots were prepared using MATLAB (version R2019a).

5.3 Virus Comparison

To see if our corrected viruses were also similar, the virus VSF (VSF_{Virus}) from the North Atlantic and GOM samples were measured (figure 5.2). The VSF_{Virus} was

calculated for both regions. The virus VSF from both regions are overlapping and are not significantly different (one-way ANOVA; p-value > 0.05). This gives us confidence that our measured virus VSF after correction is an accurate representation of the virus VSF in the samples.

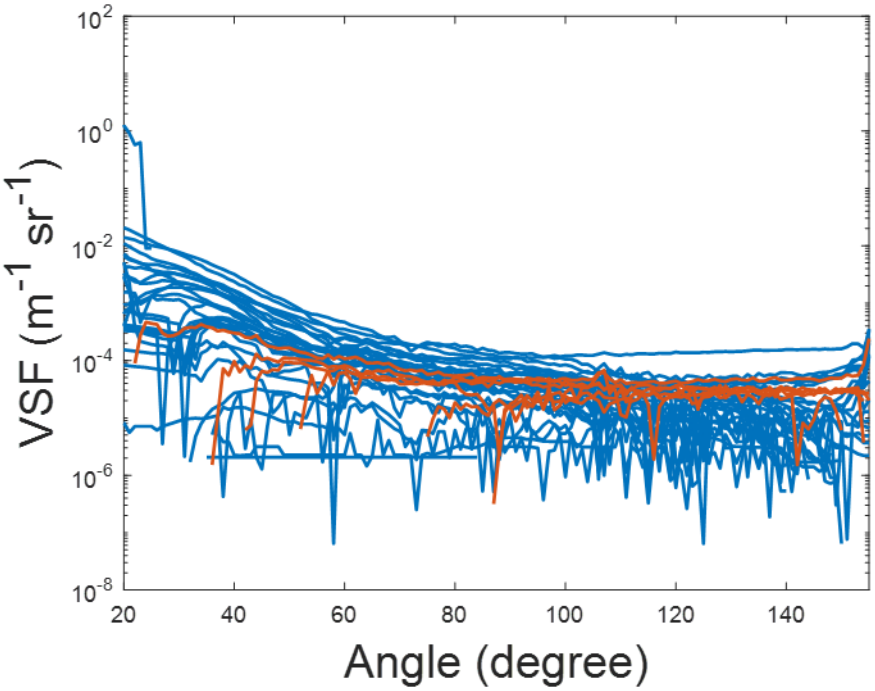

Figure 5.2 *North Atlantic and GOM virus VSF comparison*

A semilog plot (y-axis has a base-10 logarithmic scale) that shows the VSF values in GOM virus fraction (red lines) and NA virus fraction (blue lines). The blue lines represents the VSFs of the virus fraction in the North Atlantic. The red lines represents the VSFs of the virus fraction in the GOM. Visually, the lines slopes and values look similar from 90-160° and are not statistically significantly different (one-way ANOVA; p-value > 0.05). Semilog plot was prepared using MATLAB (version R2019a).

The only previous study that investigated the contribution of viruses to backscatter concluded that marine viruses have no significant contribution to the total backscatter of seawater (Balch et al. 2000). Therefore, if we compare the VSF_{Virus} of the

current study (NA) to the results of Balch et al. (2000), we find that the Balch et al. (2000) cultures had a higher VSF than what was measured in the NA (Figure 5.3 A). Balch et al. (2000) only measured at certain angles, whereas this current experiment measured every 1°. A higher VSF is likely due to a higher concentration of viruses in Balch et al. (2000) than what was measured in the NA. Balch et al. (2000) mentioned in their study that the "four types of phage were propagated to concentrations of 10^{10} to 10^{12} viruses mL^{-1}". The virus concentrations that were removed from filtration in the North Atlantic ranged from $4.4x10^{6}$ to $7.9x10^{7}$ viruses mL^{-1}. The concentrations that Balch et al. (2000) used were several magnitudes higher than the concentrations observed in the North Atlantic. The difference in concentration is likely the reason for the differences in the VSF of viruses.

Scaling the VSFs by abundance displays the cross-sectional scattering of the particles being measured (Figure 5.3 B). When examining the cross-sectional scattering of both the NA samples and the Balch cultures, the Balch cultures are comparable to or lower than the NA samples. This suggests that the viruses in the NA are larger than what was measured in the Balch experiment, which is expected due to the variability of marine viruses in the natural environment. However, it is expected to see Balch's cultures to be overlapping in the lower end of the NA measurements as the NA would include viruses similar in size to what Balch measured, as well as larger viruses.

The abundance that the NA samples were scaled by was the virus abundance and not the overall particle abundance. Since there are particles other than viruses that were removed with filtration in this fraction, they could also contribute to the VSF in this fraction. This could create discrepancies with the cross-sectional scattering of the viral-

sized particles in the NA, resulting in a larger cross-sectional scattering. Extracting the viruses, similarly to Balch et al. (2000), to separate the viruses from the DOM would bridge the gap in understanding the virus and DOM's contribution to the optical scattering in the dissolved fraction.

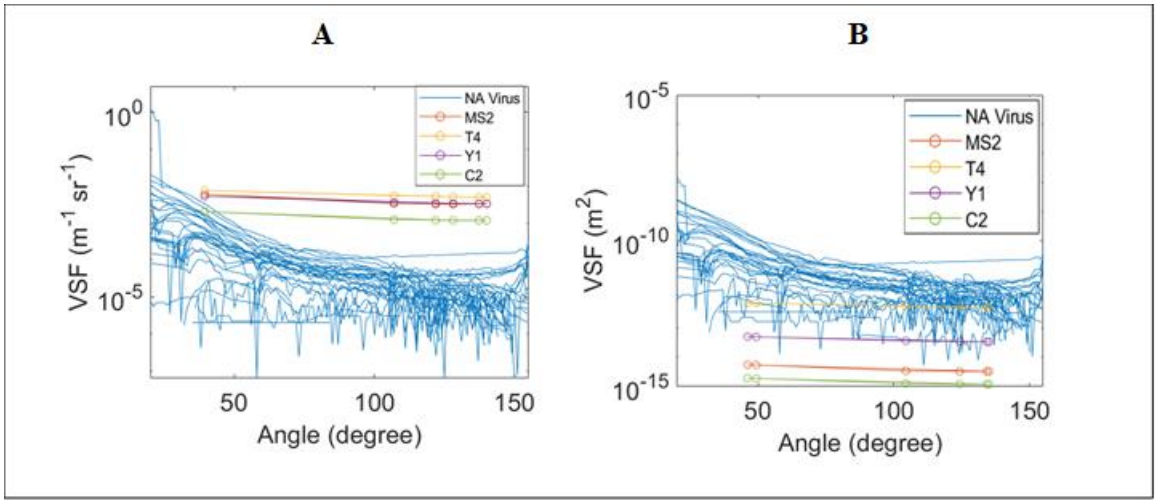

Figure 5.3 *Balch comparison*

Semilog plots (y-axis has a base-10 logarithmic scale) that shows the VSF values in the NA virus fraction compared to Balch et al. (2000) measured virus VSF's. The solid blue lines represents the VSFs of the virus fraction in the North Atlantic. The red, yellow, purple, and green lines represents the VSF of the viruses obtained from Balch et al. (2000). The Balch cultures were measured at specific angles, indicated by the circles. The NA samples were measured in 1° increments. Visually, the lines slopes look similar, but the virus VSF's obtained from Balch are shifted upwards, meaning that the concentration of viruses are higher than in the NA samples (A). FCM data reveals that Balch et al. did indeed use a higher concentration of viruses in their experiment that in this present study. When the VSFs of the Balch and NA are scaled based on each samples or cultures concentration, this shows the cross sectional scattering. The Balch cultures are lower or comparable to the NA cross section scattering (B). Semilog plots were prepared using MATLAB (version R2019a).

CHAPTER VI – FUTURE IMPROVEMENTS

To expand on the results of the current study, we would recommend that subsequent studies include additional measurements to further characterize the influence of DOM on the backscatter of the dissolved fraction. Additional measurements could include dissolved organic matter (DOM), specifically dissolved organic carbon (DOC), colored dissolved organic carbon (CDOM), and fluorescent dissolved organic carbon (FDOM), which would be beneficial to examine.

The optical properties of dissolved organic matter (DOM) have been studied as it influences the optical properties of seawater. DOM consists of many types of organic matter such as colored dissolved organic matter (CDOM), and dissolved organic carbon (DOC) (Stedmon et al. 2015). According to Coble (2007), "the optical properties of CDOM provide information on both the amount of material present and the chemical properties of the bulk sample, which undergo change due to chemical, biological, and physical processes,". DOM can influence the optical properties of seawater, and contribute to the missing backscatter.

Biological processes such as phytoplankton grazing and viral interactions can regulate the concentration of CDOM in the water column (Siegel et al. 2002). In addition, Steinberg et al. (2004) found that phytoplankton excretions introduced CDOM into the water column in the open ocean. Considering virus and phytoplankton abundance and activity in the North Atlantic, it is possible that their interactions will significantly influence CDOM into the water column, and thus influence light scattering.

Not all CDOM fluoresces, so FDOM measurements are a useful optical marker for DOM dynamics in studying humic-like (refractory DOM) and protein-like (amino

acids) substances (Coble 2007; Stedmon et al. 2015). FDOM can provide information on changes in CDOM from the mixing of water masses, resulting in dilution or combination of organic material, or biological processes, such as degradation or production, during a bloom due to new visible peaks (Coble 2007). Previous studies have found that viral lysates contain a higher amount of amino acids and labile (protein) DOM than algal exudates (Lønborg, Christian; Middelboe, Mathias; Brussaard; Corina 2013). This suggests that viral activity produces a strong FDOM signal from the viral-produced DOM, making it worthy of looking at the contribution. With an approximation of 1023 viral infection min-1 in the ocean, viruses actually may contribute a significant amount of FDOM in the natural environment (Suttle 2007). Specifically, eleven peaks are worth observing following previous research methods (Lønborg et al. 2013; Xiao et al. 2021). Nine different peaks were observed previously corresponding to common peaks of humic-like (Peaks A, C2, M, C4, C, and C3) and protein-like (Peaks T, C1, and C5) components, following Xiao et al. (2021). Lønborg et al. (2013) also analyzed two other peaks (Peaks L1 and L2). Table A.2 shows peak specifics. Measuring the FDOM would potentially provide information on virus activity in seawater.

DOC is an important and dynamic component of DOM, which is controlled by the balance between the production of phytoplankton and the consumption of bacteria (Maranger and Bird 1995; Teira et al. 2003). As viruses liberate intracellular material during lysis, they can also influence DOC dynamics (Lønborg et al. 2013). DOC is used by bacteria and transformed into bacterial biomass, increasing bacterial production (Maranger and Bird 1995). With the consumption of bacteria by grazers, this

remineralized DOC can be utilized back into the marine food web via the microbial loop (Maranger and Bird 1995; Carlson et al. 1999).

Previous studies have found that 30-50% of dissolved organic carbon is composed of marine colloids (Benner et al. 1992; Guo et al. 1994). Stramski and Woźniak (2005) modeled the scattering by colloidal particles using measured concentrations and size distributions, which indicated that small colloid particles (sized between 0.01 – 0.2 μm) contribute 44% at 350 nm and 19% at 750 nm to the average total colloidal backscattering. Sharp (1973) found that there was 8% of the total organic carbon in the 0.025-0.8 μm size fraction and 16% in the 0.003-0.8 μm size fraction. This suggests that DOC could contribute more backscatter than what was measured in Stramski and Woźniak (2005).

Measuring the DOC in the dissolved and ULMW DOM (<30 kDa) fractions has the potential to provide information on the weight (HMW or LMW) and types of DOC that contribute to the backscatter in these fractions. DOC samples should be taken immediately with the correct use of filters. According to Carlson et al. (1999), “untreated filters initially leach a measurable amount of DOC, thereby requiring thorough flushing of at least 2 L of Nano pure water and 0.5 L of sample water prior to collecting the filtrate”. In addition, Carlson et al. (1999) stated that the filters were changed every 5 L of the sample to minimize DOC released from POC retained on the filter.

CHAPTER VII – CONCLUSION

To address the potential for viruses to contribute to the optical backscatter the light scattering properties of the dissolved (<0.2 µm) and ULMW DOM (<30 kDa) fractions of seawater, these fractions light scattering properties were compared. The results of the backscatter averaged from angles 90-110° ($\beta_{(100)}$) revealed a significantly higher backscatter in the dissolved fraction than the ULMW DOM fraction (t-test; p-value < 0.05). FCM was then used to supplement the scattering properties with virus abundance. The FCM data showed that a significant number of viruses were removed in the ULMW DOM fraction. The backscatter contributed from the virus fraction (dissolved – ULMW DOM) showed that the backscatter varied with depth and latitude.

The percent contribution of virus-sized particles on the scattering measured in the dissolved fraction ($\%\beta_{Virus}$) revealed that the percent contribution varies (averaging ~50%) and is a significant contribution to the "missing backscatter" in both the NA and GOM experiments. The relationship between the $\%\beta_{Virus}$ and percent virus removal displayed a negative relationship in the NA and GOM experiments. When comparing this study's measured viral-sized particle backscatter to that of previous experiments that measured viral backscatter from cultures, this study's backscatter was higher than that of the previous experiment (Balch et al. 2000). The results of the negative relationship between the %βVirus and percent virus removal and the higher VSF of the NA to the Balch experiment may indicate that the concentration of non-virus particles affected the results of this experiment.

The outcome of these analyses has evaluated marine virus contribution to the missing backscatter. This experiment reveals that viral-sized particles contribute a

significant amount of the missing backscatter in the dissolved fraction of seawater. The various types of data collected on the STRATIPHYT-21 and Pre-PACE cruises allow for a broader knowledge of marine viruses and their contribution to optical scattering and open a completely new realm to study viruses from space.

APPENDIX A

Table A.1 *Station details STRATIPHYT-21 cruise with R/V Pelagia*

Station number	**Date**	**Time (UTC)**	**Latitude (°N)**	**Longitude (°W)**
1	14/02/2021	6:04:53	21.02405	25.88823
2	15/02/2021	6:12:19	18.99967	26.00055
3	16/02/2021	6:28:26	16.99991	26.00007
4	18/02/2021	6:28:35	15.00007	25.99998
5	21/02/2021	6:32:30	21.00011	25.99971
6	22/02/2021	6:28:31	23.00037	26.00026
7	23/02/2021	6:31:35	24.99969	25.9997
8	25/02/2021	6:30:43	26.99963	25.99992
9	26/02/2021	6:29:38	28.99977	26.00044
10	27/02/2021	6:28:58	31.33334	26.00024
11	28/02/2021	6:29:52	33.66691	25.99965
12	01/03/2021	6:31:19	35.00023	26.00042

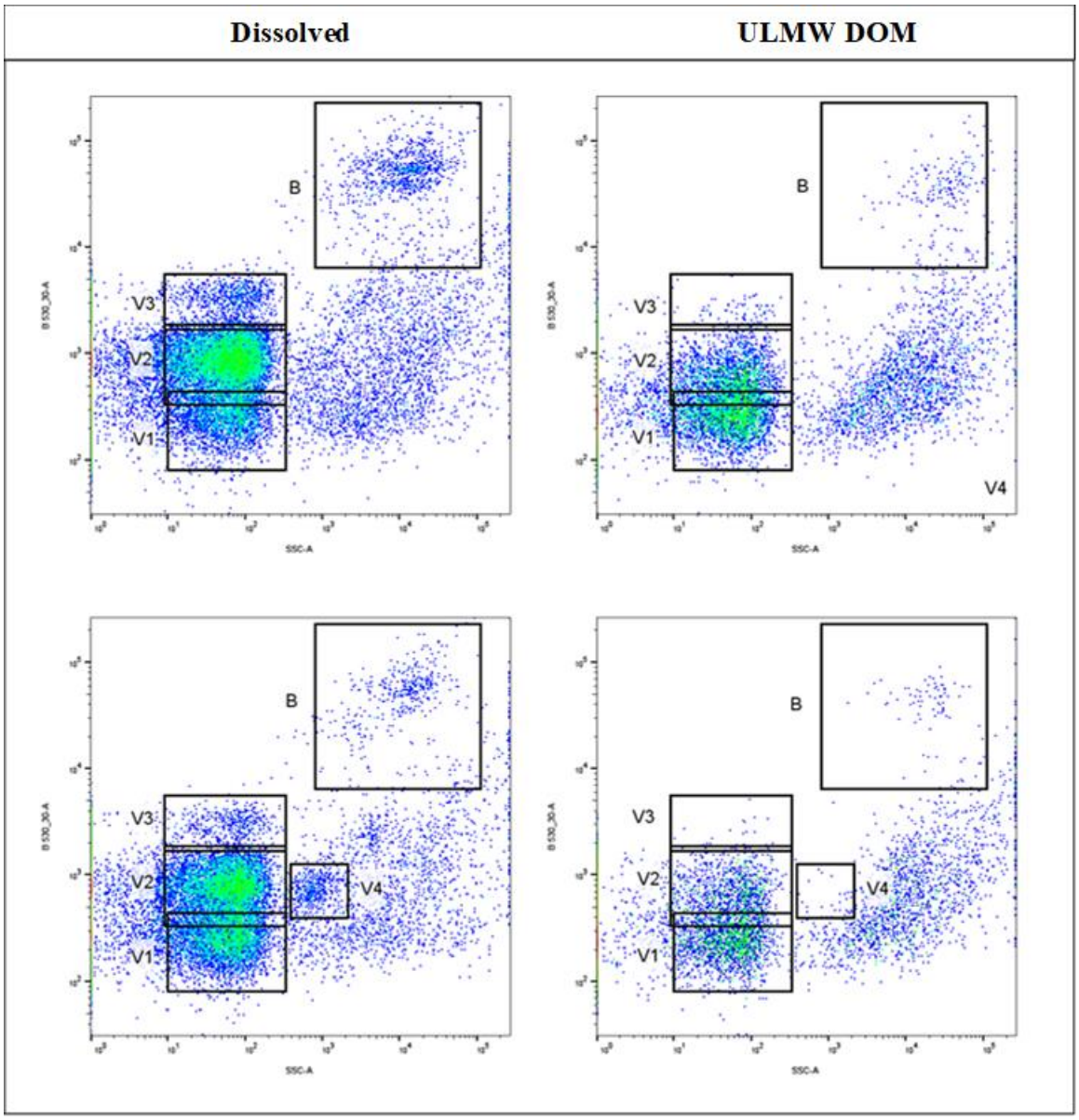

Figure A.1 *Dissolved and ULMW DOM FCM*

A cytograph showing virus populations and removal of bacteria in samples. V1, V2, and V3 represent the three bacteriophage virus populations. V4 represents one population of an algal virus. B represents the bacteria that are in the samples. The top left image shows the dissolved FCM data showing that there are three distinct virus populations and a bacteria population. The top right image is the sample's respective ULMW DOM FCM data showing that the bacteria and the third virus population have been removed by filtration. The bottom left image shows a different Dissolved sample FCM data showing an algal virus population present. The bottom right image shows that the algal virus population has been removed with filtration. The figure panels have been prepared using FlowJo (version 10.8.1).

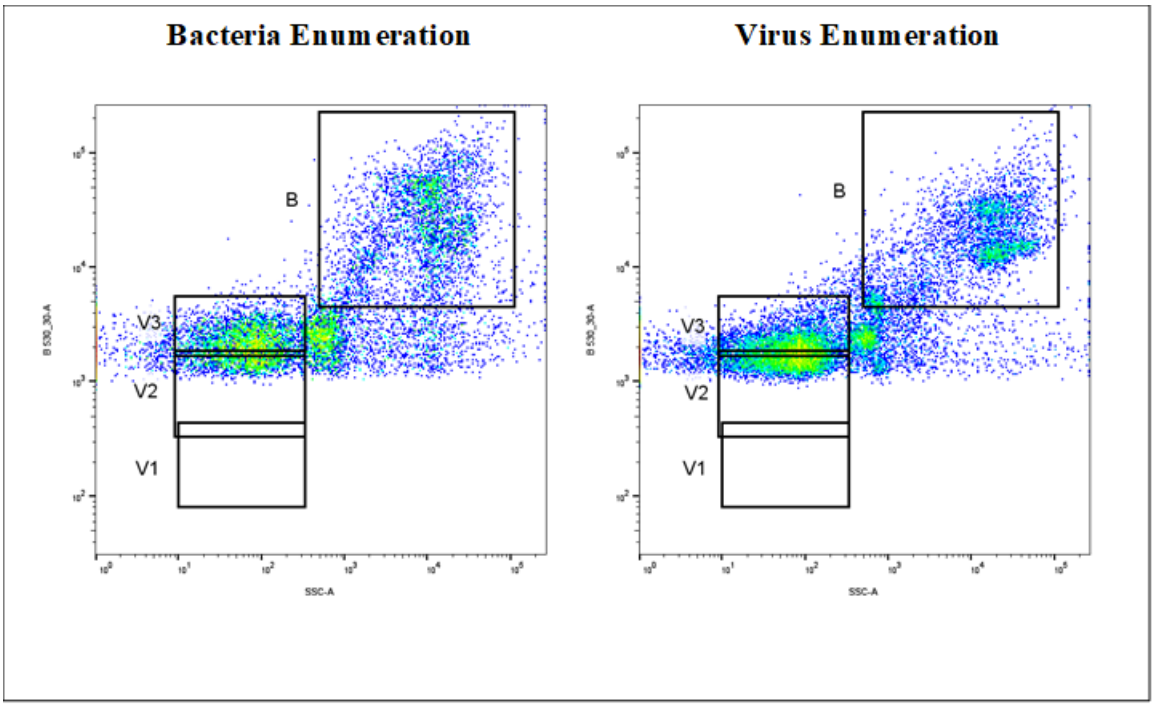

Figure A.2 *Bacteria FCM*

FCM graph showing bacteria populations with two different fixation methods. Threshold is set to 1200, the bacteria population is labelled B. Left graphs shows the sample treated with the bacteria enumeration method, and the right graph shows a sample treated with the virus enumeration method. The virus enumeration method has a higher yield of bacteria fluorescing. Figure panels have been prepared using FlowJo (version 10.8.1).

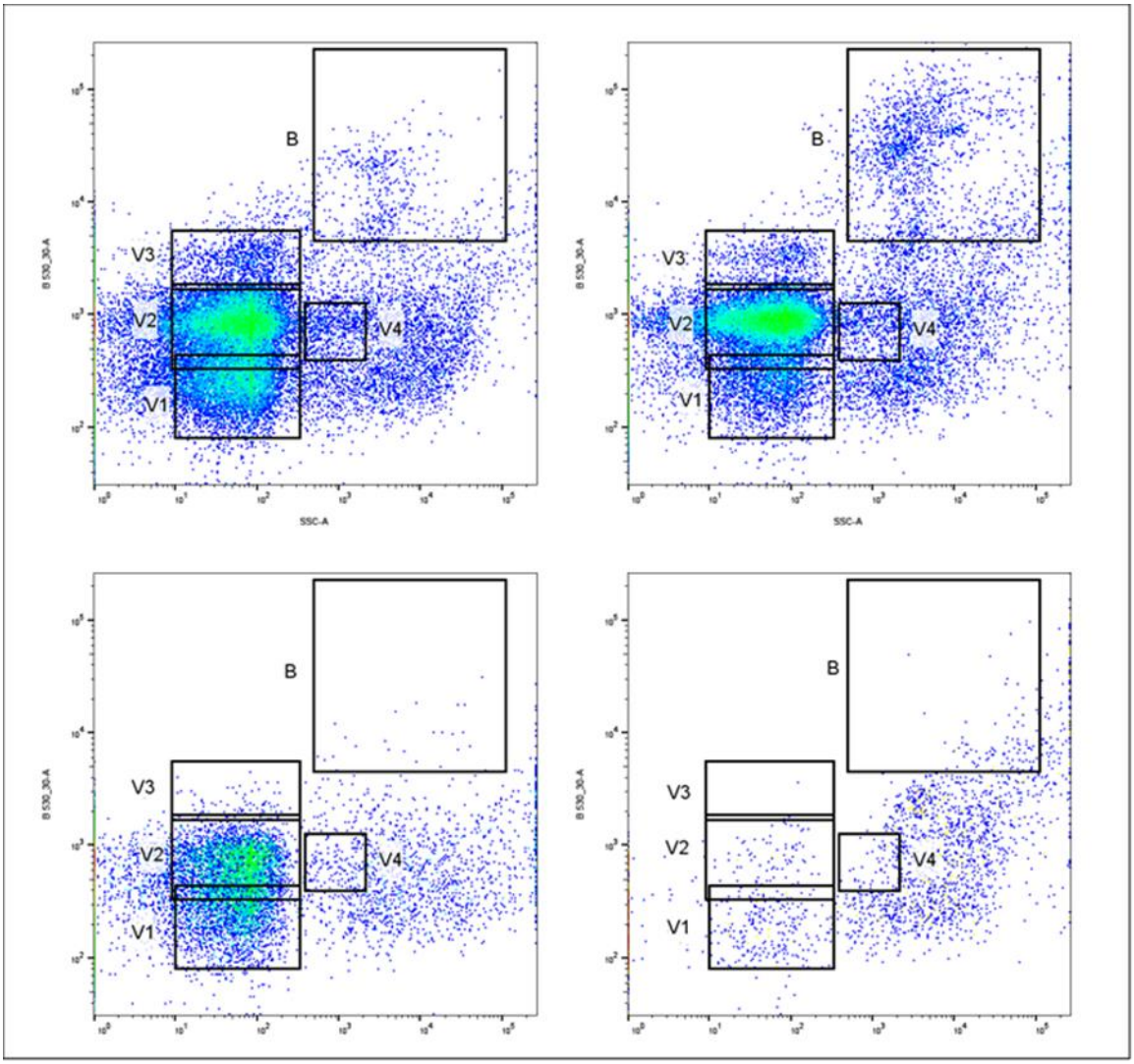

Figure A.3 *FCM of GOM samples*

A cytograph of the four fractions in the GOM case study. V1, V2, and V3 represent the three bacteriophage virus populations. V4 represents an algal virus population. B represents the bacteria populations in the sample. The top left graph (A) is fraction A, which is the dissolved fraction when the sample was collected. The top right graph (B) is fraction B, which is the dissolved fraction after being held in non-ideal conditions. The bottom left graph (C) is fraction C, which is the dissolved fraction after being held in non-ideal conditions and filtered through a 0.2 µm filter again. Lastly, the bottom right graph (D) is fraction D, which is the sample that was held in non-ideal conditions, filtered through a 0.2 µm filter, and now filtered through a 30 kDa filter. Bacteria were still present in the sample after the first filtration and multiplied after being held in non-ideal conditions. The bacteria were filtered out with additional filtration and viruses were filtered out with 30 kDa filtration. Figure panels were prepared using FlowJo (version 10.8.1).

Table A.2 *Observed FDOM peaks*

Peaks	Classification	Excitation (λ)	Emission (λ)
A	Humic-like	250	466
C2	Humic-like	255	456
M	Humic-like	335	404
C4	Humic-like	325	396
C	Humic-like	355	450
C3	Humic-like	<250	368
T	Protein-like	270	342
C1	Protein-like	275	332
C5	Protein-like	275	300
L1 (Lønborg)	Humic-like	320	410
L2 (Lønborg)	Protein-like	280	320

A total of 11 peaks were observed. The peaks describe the title of the peaks used while the classification of the peaks describes what the peaks were associated with (either protein-like or humic-like). Each peak is shown with its respective excitation and emission wavelength. Humic-like peaks A, C2, M, C4, C, and C3 and protein-like peaks T, C1, and C5 are peaks previously observed by Xiao et al. (2021). Humic-like peak L1 and protein-like peak L2 are peaks previously observed in Lønborg et al. (2013).

REFERENCES

Balch, William M.; Vaughn, James; Novotny, James; Drapeau, David T.; Vaillancourt, Robert; Lapierre, Janeen; Ashe, A. 2000. Light scattering by viral suspensions. Limnology and Oceanography **45**: 492–498. DOI: 10.4319/lo.2000.24.2.0492

Benner, R., J. D. Pakulski, M. McCarthy, J. I. Hedges, and P. G. Hatcher. 1992. Bulk chemical characteristics of dissolved organic matter in the ocean. Science **255**: 1561-1564. DOI:10.1126/science.255.5051.1561

Bracher, A., H. A. Bouman, R. J. W. Brewin, et al. 2017. Obtaining Phytoplankton Diversity from Ocean Color: A Scientific Roadmap for Future Development. Frontiers in Marine Science **4**: 55. doi:10.3389/fmars.2017.00055

Bratbak, G., M. Heldal, T. F. Thingstad, B. Riemann, and O. H. Haslund. 1992. Incorporation of viruses into the budget of microbial C-transfer. A first approach. Mar. Ecol. Prog. Ser. **83**: 273–280. DOI: 10.3354/meps083273

Brussaard, C. P. D., S. W. Wilhelm, F. Thingstad, et al. 2008. Global-scale processes with a nanoscale drive: the role of marine viruses. ISME Journal **2**: 575–578. DOI:10.1038/ismej.2008.31

Carlson, C. A., N. R. Bates, H. W. Ducklow, and D. A. Hansell. 1999. Estimation of bacterial respiration and growth efficiency in the Ross Sea, Antarctica. Aquatic Microbial Ecology **19**: 229–244. DOI: 10.3354/ame019229

Castberg, T., A. Larsen, R. A. Sandaa, et al. 2001. Microbial population dynamics and diversity during a bloom of the marine coccolithophorid Emiliania huxleyi (Haptophyta). Mar. Ecol. Prog. Ser. **221**: 39–46. DOI: 10.3354/meps221039

Coble, P. G. 2007. Marine Optical Biogeochemistry: The Chemistry of Ocean Color. Chem. Rev. **107**: 402–418. DOI: 10.1021/cr050350+

Dickey, T. D., and P. G. Falkowski. 2002. Solar energy and its biological-physical interactions in the sea. Chapter 10, The Sea **12**: 401-440.

Guo, L., P. H. Santschi, and C. H. Coleman. 1994. The distribution of colloidal and dissolved organic carbon in the Gulf of Mexico. Marine Chemistry **45**: 105-119. DOI: 10.1016/0304-4203(94)90095-7

Lønborg, C., M. Middelboe, and C. P. D. Brussaard. 2013. Viral lysis of *Micromonas pusilla*: impacts on dissolved organic matter production and composition. Biogeochemistry **116**: 231–240. DOI: 10.1007/s10533-013-9853-1

Maranger, R., and D. F. Bird. 1995. Viral abundance in aquatic systems: a comparison between marine and fresh waters. Mar Ecol. Prog. Ser. **121**: 217–226. DOI: 10.3354/meps121217

Marie, D., C. P. D. Brussaard, R. Thyrhaug, G. Bratbak, and D. Vaulot. 1999. Enumeration of Marine Viruses in Culture and Natural Samples by Flow Cytometry. Applied Environmental Microbiology **65**: 45–52. DOI: 10.1128/aem.65.1.45-52.1999

Marie, D., F. Partensky, S. Jacquet, and D. Vaulot. 1997. Enumeration and Cell Cycle Analysis of Natural Populations of Marine Picoplankton by Flow Cytometry Using the Nucleic Acid Stain SYBR Green I. Applied Environmental Microbiology **63**: 186–193. DOI: 10.1128/aem.63.1.186-193.1997

Mobley, C. D. 2022. The Oceanic Optics Book. DOI: 10.25607/OBP-1710

Morel, A., and Y.-H. Ahn. 2008. Optics of heterotrophic nanoflagellates and ciliates: A tentative assessment of their scattering role in oceanic waters compared to those of bacterial and algal cells. Journal of Marine Research **49**: 177–202. DOI: 10.1357/002224091784968639

Sharp, J. H. 1973. SIZE CLASSES OF ORGANIC CARBON IN SEAWATER. Limnology and Oceanography **18**: 441–447. DOI: 10.4319/lo.1973.18.3.0441

Siegel, D. A., S. Maritorena, N. B. Nelson, D. A. Hansell, and M. Lorenzi-Kayser. 2002. Global distribution and dynamics of colored dissolved and detrital organic materials. Journal of Geophysical Research: Oceans **107**: 21-1-21-14. DOI: 10.1029/2001jc000965

Stedmon, Colin A. and U. Nelson, Norman B. 2015. The Optical Properties of DOM in the Ocean, p. 481–508. *In* Biogeochemistry of Marine Dissolved Organic Matter.

Steinberg, D. K., N. B. Nelson, C. A. Carlson, and A. C. Prusak. 2004. Production of chromophoric dissolved organic matter (CDOM) in the open ocean by zooplankton and the colonial cyanobacterium *Trichodesmium* spp. Mar. Ecol. Prog. Ser. **267**: 45–56. DOI: 10.3354/meps267045

Stramski, D., E. Boss, D. Bogucki, and K. J. Voss. 2004. The role of seawater constituents in light backscattering in the ocean. Progress in Oceanography **61**: 27–56. doi:10.1016/j.pocean.2004.07.001

Stramski, D., and D. A. Kiefer. 1991. Light scattering by microorganisms in the open ocean. Progress in Oceanography **28**: 343–383. DOI: 10.1016/0079-6611(91)90032-H

Stramski, D., and S. B. Woźniak. 2005. On the role of colloidal particles in light scattering in the ocean. Limnology and Oceanography **50**: 1581–1591. DOI: 10.4319/lo.2005.50.5.1581

Suttle, C. A. 2007. Marine viruses - Major players in the global ecosystem. Nature Reviews Microbiology **5**: 801–812. DOI: 10.1038/nrmicro1750

Teira, E., M. J. Pazó, M. Quevedo, M. v. Fuentes, F. X. Niell, and E. Fernández. 2003. Rates of dissolved organic carbon production and bacterial activity in the eastern North Atlantic Subtropical Gyre during summer. Mar. Ecol. Prog. Ser. **249**: 53–67. DOI: 10.3354/meps249053

Weinbauer, M. G. 2004. Ecology of prokaryotic viruses. FEMS Microbiology Review **28**: 127–181. DOI: 10.1016/j.femsre.2003.08.001

Wigington, C. H., D. Sonderegger, C. P. D. Brussaard, and others. 2016. Re-examination of the relationship between marine virus and microbial cell abundances. Nature Reviews Microbiology **1**. 15024. DOI: 10.1038/nmicrobiol.2015.24

Wommack, K. E., and R. R. Colwell. 2000. Virioplankton: Viruses in Aquatic Ecosystems. Microbiology and Molecular Biology Reviews **64**: 69–114. DOI: 10.1128/mmbr.64.1.69-114.2000

Xiao, X., W. Guo, X. Li, et al. 2021. Viral Lysis Alters the Optical Properties and Biological Availability of Dissolved Organic Matter Derived from *Prochlorococcus* Picocyanobacteria. Applied Environmental Microbiology **87**: 1–19. DOI: 10.1128/AEM.02271-20

Zhang, X., L. Hu, Y. Xiong, Y. Huot, and D. Gray. 2020. Experimental Estimates of Optical Backscattering Associated With Submicron Particles in Clear Oceanic Waters. Geophysical Research Letters **47**. DOI: 10.1029/2020GL087100